



Evaluating immune cells in physiological settings:

Studying the neonatal immune
landscapes and the effect of fever-
range temperatures on T-cell
differentiation

Ira Phadke

**Indian Institute of Science Education and Research, Pune
(IISER-P)**

Department of Biology

Research Mentors:

Prof. Vineeta Bal, IISER Pune

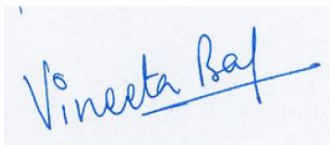
Prof. Satyajit Rath, Agharkar Research Institute Pune

TABLE OF CONTENTS

CERTIFICATE.....	2
DECLARATION.....	3
ABSTRACT	4
ACKNOWLEDGEMENTS	5
LIST OF FIGURES AND TABLES	6
OVERVIEW.....	7
PART I: ANALYSIS OF NEONATAL LEUCOCYTE SUBSET LANDSCAPES	8
INTRODUCTION	9
“The thin-fat Indian”	9
Why are dietary nutrients important?	9
Nutriepigenomics and fetal programming	10
PBMCs as a proxy for immune system development	11
MATERIALS AND METHODS	12
RESULTS	20
DISCUSSION	32
PART II: EFFECT OF TEMPERATURE ON T CELL DIFFERENTIATION	36
INTRODUCTION	37
Fever initiation: Common to endotherms and ectotherms	37
Fever boosts the innate immune arm	37
Fever and T cell responses	38
Temperature sensing mechanisms in T cells	39
MATERIALS AND METHODS	41
RESULTS	44
DISCUSSION.....	47
BIBLIOGRAPHY	48

CERTIFICATE

This is to certify that this dissertation entitled “Evaluating immune cells in physiological settings: Studying the neonatal immune landscapes and the effect of fever-range temperatures on T-cell differentiation” towards the partial fulfilment of the BS-MS dual degree programme at the Indian Institute of Science Education and Research, Pune represents study/work carried out by Ira Phadke at IISER Pune under the supervision of Prof. Vineeta Bal, Visiting Faculty, Department of Biology during the academic year 2017-2018.



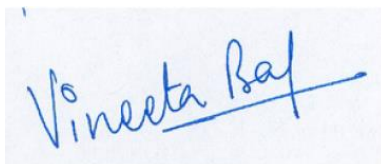
Supervisor's Signature



Student's Signature

DECLARATION

I hereby declare that the matter embodied in the report entitled “Evaluating immune cells in physiological settings: Studying the neonatal immune landscapes and the effect of fever-range temperatures on T-cell differentiation” are the results of the work carried out by me at the Department of Biology, IISER-Pune, under the supervision of Prof. Vineeta Bal and the same has not been submitted elsewhere for any other degree.

A handwritten signature in blue ink that reads "Vineeta Bal" with a horizontal line underneath.

Supervisor's Signature

A handwritten signature in blue ink enclosed within a rectangular box. The signature is partially obscured by a horizontal line.

Student's Signature

ABSTRACT

The immune network is modulated by an n-dimensional matrix of genetic, epigenetic and environmental factors. In neonates, development occurs in an immunologically sterile environment. Their immune landscape is modelled predominantly by genetic and ethno-geographical factors. These inherent variations give rise to populations of immune subsets that are both tightly and loosely regulated. One such human population study, from 6 villages near Pune, showed interesting trends in frequencies of B, T, and innate cell subsets. Moreover, the data also presented correlations between frequencies of immune subsets that developmentally belong to distinct lineages, therefore raising questions about probable “common” interacting pathways. Conversely, post infection in vertebrates, a febrile response is generated on immunological challenge. Previous reports have demonstrated that hyperthermia augments immune responses of the innate and adaptive arms. However, the effect of temperature on T-cell fate determination is not known. The data presented here, suggests that the Th2 response is likely to be affected more significantly than the Th1 response at raised temperatures. Further quantitative studies need to be undertaken to decipher the molecular players that sense temperature fluctuations and activate downstream signaling in this pathway.

LIST OF FIGURES AND TABLES

List of Figures

FIGURE 1: FLOW CYTOMETRIC GATING STRATEGIES FOR B CELL SUBSETS...	15
FIGURE 2: FLOW CYTOMETRIC GATING STRATEGIES FOR INNATE CELL SUBSETS	16
FIGURE 3: FLOW CYTOMETRIC GATING STRATEGIES FOR T AND NKT CELL SUBSETS	17
FIGURE 4: FLOW CYTOMETRIC GATING STRATEGIES FOR TREG CELL SUBSETS	18
FIGURE 5: MAJOR SUBSET FREQUENCY DISTRIBUTIONS.....	23
FIGURE 6: B CELL SUBSET FREQUENCY DISTRIBUTIONS	24
FIGURE 7: CD4 T CELL SUBSET FREQUENCY DISTRIBUTIONS	25
FIGURE 8: CD8 T CELL SUBSET FREQUENCY DISTRIBUTIONS	26
FIGURE 9: T CELL SUBSET FREQUENCY DISTRIBUTIONS	27
FIGURE 10: MONOCYTE AND DC SUBSET FREQUENCY DISTRIBUTIONS	28
FIGURE 11: COEFFICIENT OF VARIATION OF IMMUNE SUBSET FREQUENCIES	29
FIGURE 12: CORRELATIONS BETWEEN CORD BLOOD IMMUNE SUBSET FREQUENCIES	30
FIGURE 13: COMPARISON OF GATA3 MRNA LEVELS IN 37°C AND 40°C JURKAT CELLS.....	44
FIGURE 14: REPRESENTATIVE GEL IMAGE FOR GATA3 PCR USING JURKAT CDNA	45
FIGURE 15: COMPARISON OF TBET MRNA LEVELS IN 37°C AND 40°C JURKAT CELLS	46
FIGURE 16: REPRESENTATIVE GEL IMAGE FOR TBET PCR USING JURKAT CDNA	46

List of Tables

TABLE 1: FLOW CYTOMETRIC PHENOTYPIC MARKERS USED	13
TABLE 2: THE PARTICIPANT POPULATION CHARACTERISTICS	20
TABLE 3: REFERENCE STATISTICS FOR FREQUENCIES OF IMMUNE SUBSETS	21

ACKNOWLEDGEMENTS

“Although the world looks messy and chaotic, if you translate it into the world of numbers and shapes, patterns emerge, and you start to understand why things are the way they are.” – Marcus du Sautoy

This has been a fascinating experience. I have grown to learn, appreciate and understand many aspects of science, as a community and as a subject. Firstly, I would like to extend my gratitude to my supervisors, Prof. Vineeta Bal and Prof. Satyajit Rath for ‘priming’ me to appreciate immunology and helping me overcome roadblocks. Next, I would like to thank my TAC member, Dr. Jeet Kalia for his patience and inputs during my mid-year presentation. I would also like to thank members of Dr. Prasenjit Guchhait’s lab in Regional Centre for Biotechnology, Faridabad, especially Angika Bhasym and Amrita Ojha for helping me with the flow cytometric analysis that formed an integral part of my thesis. I would also like to thank my lab members, Dr. Sushama Rokade and Dr. Gauri Mirji for helping me troubleshoot towards the end of my project. Further, I would like to extend a special thanks to the members of Sanjeev Galande, Gayathri Pananghat and Sai Krishnan Kayarat’s lab for reagents, gel analysis, and their support. Also, I would like to thank IISER-Pune for providing me with the opportunity to carry out this project and DST-INSPIRE for my fellowship. Lastly, I am grateful to my parents, friends, and family for their constant love and support.

OVERVIEW

The vertebrate immune system orchestrates a complex set of responses in different microenvironments. The gene expression in immune cells is governed by both genetic and epigenetic factors. The composition of the immune cells in the blood, variable in an individual and population within certain limits, at any given point, plays a key role in understanding the health status of the individual. Thus, this project is looking at two aspects of the immune system in starkly different contexts.

The thesis work described here has been subdivided into two parts, in an attempt to study the immune system in real physiological conditions:

Part I: Analysis of neonatal leucocyte subset landscapes: sterile environment

This section deals with the characterization of immune cells in an immunologically sterile environment, viz, during fetal development. During intrauterine development, the baby is heavily protected from pathogens and harmful exposures, yet there are many other variables such as maternal nutrition and genome composition that produce variations among the leucocyte subsets.

Part II: Effect of Temperature on T cell differentiation: post infection

This section deals with understanding the role of fever in the differentiation of T cells. On encountering infection, one of the most common responses of the body is to reset the basal body temperature and induce whole-body fever. This rise in temperature by just a few degrees has subtle yet pronounced effects on the immune cells.

PART I: Analysis of neonatal leucocyte subset landscapes

INTRODUCTION

“The thin-fat Indian” (Yajnik et al., 2003)

A significantly large percentage of about 30% babies are born with low birth weight in India. This directly reflects poor intrauterine nourishment during neonatal development and fetal programming. These Indian babies, despite being born with low birth weight have relatively low muscle mass and more subcutaneous fat (thin-fat phenotype) as compared to their European counterparts (Yajnik et al., 2003). This central obesity and higher insulin resistance, coupled with intrauterine malnourishment predispose these babies to lifestyle disorders in the adulthood such as type 2 diabetes and cardiovascular ailments which are non-communicable diseases (NCDs) (Yajnik et al., 2008). However, the molecular mechanisms underlying fetal programming and the molecular pathways connecting intrauterine nutrient intake to NCDs like type 2 diabetes are not well understood.

Why are dietary nutrients important?

In the Pune Maternal Nutritional Study (PMNS) undertaken by Dr. Yajnik from KEM Hospital, Pune, it was established that folate and Vitamin B12, which are central players of the one-carbon metabolism (OCM) pathway regulate methylation capacity of the cell by affecting the homocysteine levels that play a role as methyl donors/acceptors (Yajnik et al., 2008)

Vitamin B12 plays a central role at the intersection of the folate and methionine cycle within the cell cytoplasm. The end product of the folate cycle, 5-CH₃-tetrahydrofolate (5-CH₃-THF) donates a methyl group to homocysteine which leads to the generation of methionine. At this step, Vitamin B12 is an essential cofactor for the enzyme, methionine synthase. Low levels or absence of Vitamin B12 traps 5-CH₃-THF resulting in an increase in homocysteine concentrations and its by-products. This has a two-fold effect on the cell metabolism. Firstly, cell toxicity builds up due to increased homocysteine concentrations, and secondly, methionine deficiency results in reduced methylation potential of the cell (Scott et al., 1999). This potentially affects DNA

methylation and thus dysregulates gene expression (Fowden et al., 2006; Choi et al., 2005). These methylation patterns if established during intrauterine fetal development could generate stable gene expression alterations that could lead to long-lasting repercussions during adult life (Fowden et al., 2005; Harding et al., 1995; Ciappio et al., 2011; Lillycrop et al., 2005).

Nutriepigenomics and fetal programming

Nutriepigenomics is a fairly new discipline that inspects the overlap between nutrition and gene expression patterns that are modelled by nutrient intake. There has been growing evidence indicating the role of nutrition in establishing and altering gene expression patterns via epigenetic mechanisms. A study undertaken by Waterland *et al.* (Waterland and Jirtle, 2003) elucidated that the offspring of genetically obese Agouti mice showed a reduction in obesity along with an alteration in their coat colour. This was achieved by introducing dietary changes in the pregnant Agouti mice, that is by feeding them with methyl supplements, thus altering the methylation status of the offspring. They further went on to show that this change in offspring phenotype was the result of promoter methylation of the Agouti gene, which led to its suppression despite inheritance from the parents. Another similar report showed that sheep fed with a Vitamin B12, folate and methionine-restricted diet before conception and during early pregnancy, produced offspring that later in adult life developed insulin resistance, high blood pressure, were heavier and produced an altered immune response. (Sinclair et al., 2007). These studies reveal the subtle yet profound effect that maternal diet has on the health status of offspring in animal models.

With increased awareness, observational studies in humans have also started emerging. One such study has been described earlier: PMNS. In this study, 700 pregnant women from six villages near Pune were monitored, and their dietary intake was measured (Vitamin B 12, folate, homocysteine levels, etc.). These measures were then correlated with the detailed anthropometry of offspring, fat-muscle body composition and insulin resistance at 6years age. The data revealed that high folate diets coupled with low Vitamin B12 intake culminated in the offspring developing higher

insulin resistance and adiposity. This demonstrated that the “thin-fat” Indian phenotype predisposes them to diseases such as type 2 diabetes (Yajnik et al., 2003, 2006, 2008).

Peripheral blood mononuclear cells as a proxy for immune system development

Several genetic and epigenetic factors regulate the composition of peripheral blood mononuclear cells (PBMCs) in humans (Huang et al., 2014; Orru et al., 2013; Evans et al., 1999; MacGillivray et al., 2014; Paparo et al., 2014). This PBMC composition is likely to be affected in neonates by the genetic factors and health status of the mother during the pregnancy. In India, detailed immunophenotyping of a population has been undertaken by a handful of groups (Prabhu et al., 2016; Rathore et al., 2015; Chan et al., 2009). These characterized immune subsets from cord blood act as a proxy for fetal development, and their distributions can be affected by a number of variables such as gene compositions, socio-economic background, geographical location, and nutritional intake, rather than direct environmental impacts, since during intrauterine development, neonates are extensively protected from pathogens and detrimental exposures.

The current study has been undertaken in an attempt to decipher the role of nutrition particularly Vitamin B12 and micronutrients in fetal programming and pregnancy outcome via a detailed OMICS analysis (transcriptome, epigenome, and genome) carried out on cord blood samples taken from the babies of the rural females from 6 villages near Pune, that were part of the PMNS project. These females received different nutrition supplements from adolescent period onwards in a randomized trial before and during the course of the pregnancy. One of the aims of this study is to evaluate the direct effect of nutritional supplementation on the neonatal immune system development and examine if the leucocyte subset distributions are affected by maternal nutritional intake. This will help us gather insight into the pathophysiology and manifestations of non-communicable diseases and may come up with effective intervention plans to prevent these NCDs.

MATERIALS AND METHODS

Study Design and Ethics Statement:

The immunophenotyping of cord blood samples was done as part of an ongoing mega inter-generational nutritional intervention trial undertaken by Dr. Yajnik from KEM hospital, Pune. The cohort comprises the babies born to rural women who as adolescent girls were a part of the Pune Maternal Nutritional Study (PMNS), and belong to six villages near Pune, Maharashtra. The KEM Hospital Ethical Committee and local village leaders granted permission to carry out this study. For each cord blood sample collected, informed consent was taken from the mothers.

The cord blood samples from babies were collected, the peripheral blood mononuclear cells (PBMCs) were isolated and stored in the freezing mix: 10% Dimethyl sulphoxide (DMSO) in fetal bovine serum (FBS) in liquid nitrogen. PBMCs from each cord blood sample were thawed, cells washed in 1x phosphate buffer saline (PBS) and divided into five equal parts and stained using four cocktails of pre-optimized concentrations of fluorophore-labeled monoclonal antibodies (eBiosciences and BD Pharmigen) and one cocktail containing a viability dye (7AAD). The cocktail compositions used for staining are as follows:

Cocktail 1: B cell subsets (To detect CD10-PECy7, CD19-V500, CD20-APC780, CD27-V450, CD38-PECy5, CD43-FITC, IgM-APC as phenotypic markers)

Cocktail 2: Innate cell subsets (To detect CD3-V500, CD11c-PECy5, CD16-PECy7, CD14-V450, CD19-V500, CD56-PE, CD123-APC, HLA DR-APC780 as phenotypic markers)

Cocktail 3: T cell and NKT cell subsets (To detect CCR7-V450, CD3-PECy5, CD4-APC780, CD8-BV510, CD45RO-PECy7, CD56-APC, iNKT-FITC, $\gamma\delta$ TCR-PE, as phenotypic markers)

Cocktail 4: Treg subsets (To detect CD4-APC780, CD8-V500, CD25-PECy5, CD39-BV421, CD45RO-PECy7, CD127-APC, FoxP3-PE, Helios-FITC as phenotypic markers)

The concentrations of antibodies added to each cocktail was pre-determined by titration and optimization. Each sample was stained for the cell surface markers with Cocktails 1, 2 and 3. For Cocktail 4, first, the cells were stained for the cell surface markers, then fixed with eBiosciences 1x Fixation/Permeabilization buffer in the dark, washed and subsequently stained for intracellular markers diluted in the eBiosciences 1x Permeabilization buffer. Then, the excess antibodies were washed off, and all the samples were resuspended in the staining buffer (1% BSA in 1x PBS) and acquired on FACS Aria III, BD Biosciences. The data analysis was done using FlowJo (TreeStar, Ashland, OR), and statistical analysis was done using GraphPad Prism software.

The data acquired was then subjected to a serial gating strategy, which was used to identify leucocyte subsets, using cell surface and intracellular markers (Table 1) within the cord blood samples along with their respective frequencies. A primary FSC-SSC gate was applied to all the cocktails (Figure 1, A) to eliminate false signals from cell clumps. Further gating strategy has been illustrated in Figure 1-4 for each cocktail separately.

Table 1: Flow cytometric phenotypic markers used to identify leucocyte subsets.

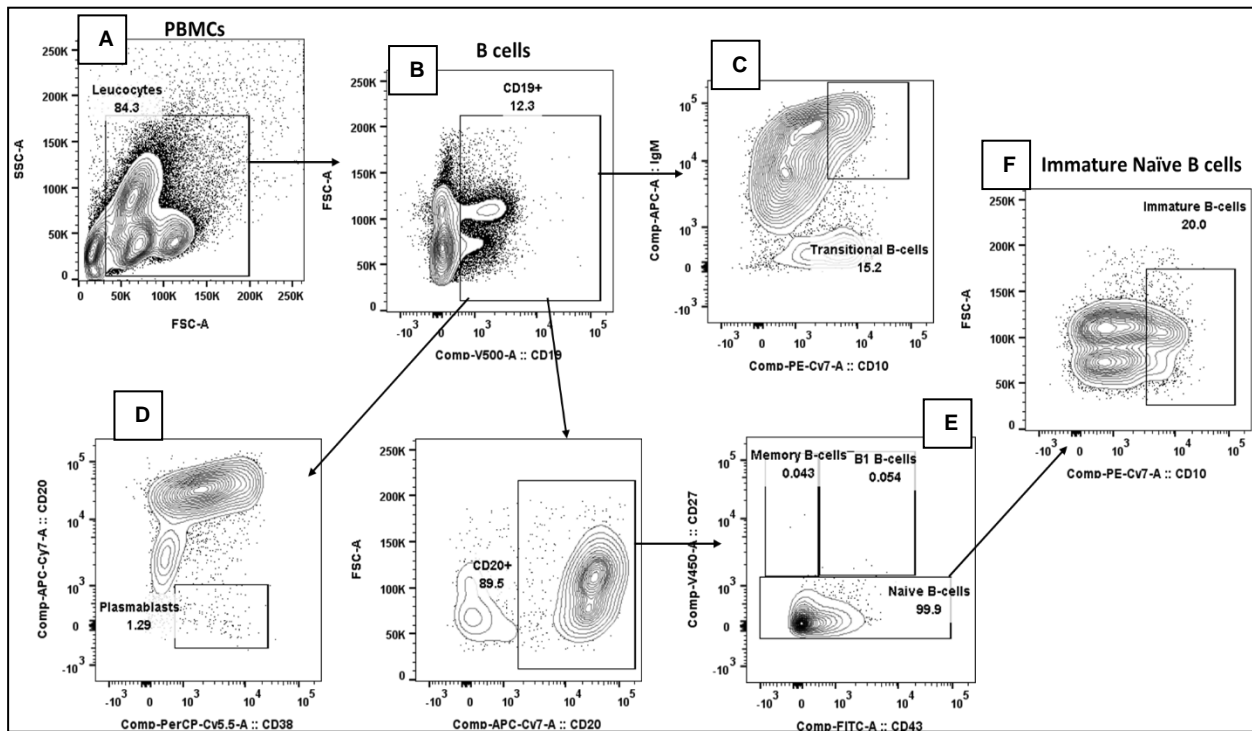
Cell subset	Phenotypic marker
Total leucocytes	FSC-SSC gate
Cocktail 1: B cell subsets	
All B cells	CD19+
All B cells (excluding plasmablasts)	CD19+CD20+
Plasmablasts	CD19+ CD20 dull CD38+
Transitional B cells	CD19+ IgM+ CD10
Memory B cells	CD19+ CD20+ CD43 dull CD27+
B1 B cells	CD19+ CD20+ CD43 bright CD27+
Naïve B cells	CD19+ CD20+ CD27 dull
Immature naïve B cells	CD19+ CD20+ CD27 dull CD10+
Cocktail 2: Innate cell subsets	
Total monocytes	CD14+ CD11c+

Classical monocytes (CM)	CD14+ CD11c+ CD16 dull
Patrolling monocytes (PM)	CD14 dull CD11c+ CD16+
Inflammatory monocytes (IM)	CD14 bright CD11c+ CD16+
Natural killers (NKs)	CD56+
Dendritic cells (DCs)	Lineage- HLA-DR bright
Myeloid DCs	Lineage- HLA-DR bright CD11c bright CD123 dull
Plasmacytoid DCs	Lineage- HLA-DR bright CD11c dull CD123+
Cocktail 3: T cell and NKT cell subsets	
Total T cells	CD3+
$\gamma\delta$ T cells	CD3+ $\gamma\delta$ TCR+
Natural Killer T cells (NKT)	CD3+ $\gamma\delta$ TCR- CD4- CD8- CD56+
Invariant NKT cells (iNKT)	CD3+ $\gamma\delta$ TCR- CD4- CD8- CD56+ iNKT+
CD4 T cells	CD3+ $\gamma\delta$ TCR- CD4+ CD8-
CD8 T cells	CD3+ $\gamma\delta$ TCR- CD8+ CD4-
Central memory CD4 T cells (CD4 CM)	CD3+ $\gamma\delta$ TCR- CD4+ CD8- CD45RO+ CCR7+
Effector memory CD4 T cells (CD4 EM)	CD3+ $\gamma\delta$ TCR- CD4+ CD8- CD45RO+ CCR7 dull
Effector memory recall CD4 T cells (CD4 EMRA)	CD3+ $\gamma\delta$ TCR- CD4+ CD8- CD45RO dull CCR7-
Naïve CD4 T cells	CD3+ $\gamma\delta$ TCR- CD4+ CD8- CD45RO dull CCR7+
Central memory CD8 T cells (CD8 CM)	CD3+ $\gamma\delta$ TCR- CD8+ CD4- CD45RO+ CCR7+
Effector memory CD8 T cells (CD8 EM)	CD3+ $\gamma\delta$ TCR- CD8+ CD4- CD45RO+ CCR7 dull
Effector memory recall CD8 T cells (CD8 EMRA)	CD3+ $\gamma\delta$ TCR- CD8+ CD4- CD45RO dull CCR7-
Naïve CD8 T cells	CD3+ $\gamma\delta$ TCR- CD8+ CD4- CD45RO dull CCR7+
Cocktail 4: Regulatory T cell subsets	

Regulatory T cells (Tregs)	CD4+ CD127 dull CD25+ Foxp3+
Activated Tregs	CD4+ CD127 dull CD25+ Foxp3+ CD45RO+ CD39+
Natural Tregs (nTregs)	CD4+ CD127 dull CD25+ Foxp3+ Helios+
Activated nTregs	CD4+ CD127 dull CD25+ Foxp3+ Helios+ CD45RO+ CD39+
Induced Tregs (iTregs)	CD4+ CD127 dull CD25+ Foxp3+ Helios-

Leucocyte subsets which were identified based on antibodies listed in cocktail 1 above are primarily B cell subsets. A representative gating strategy is shown in Figure 1.

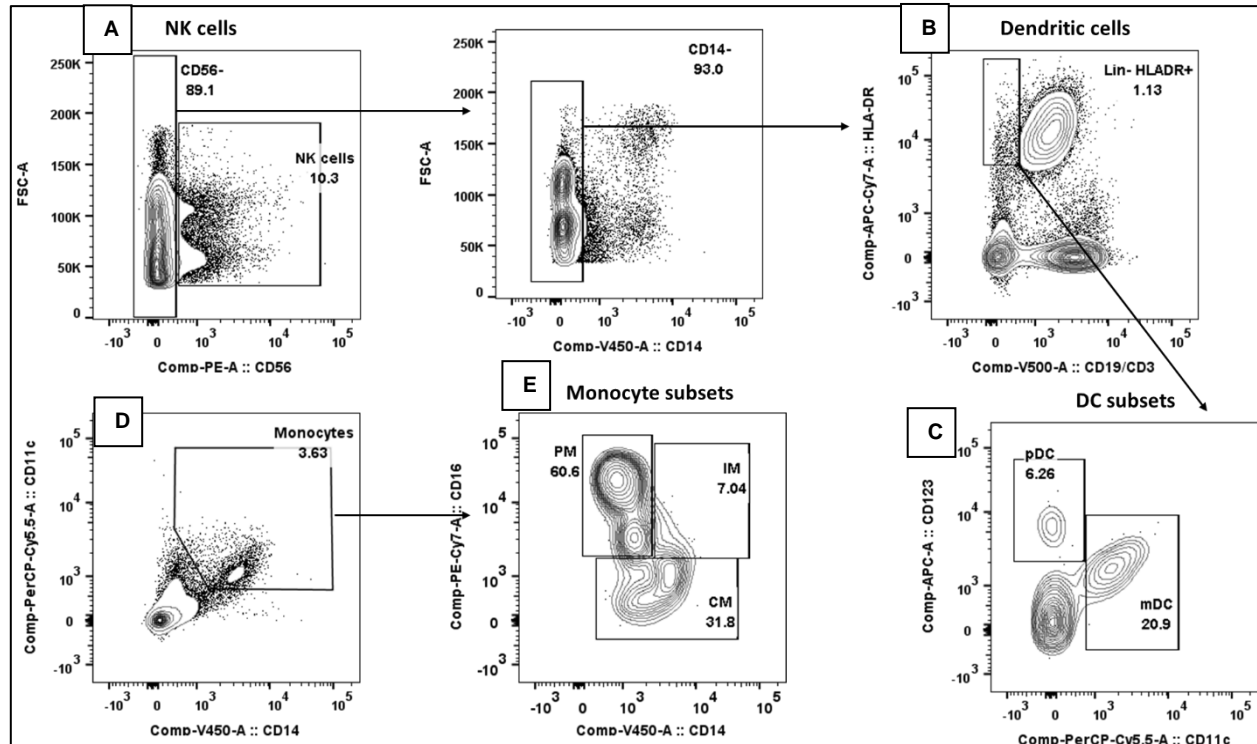
Figure 1: Flow cytometric gating strategies for B cell subsets in cord blood.



From total leucocytes [A], total B cells are identified using CD19+ [B]. Transitional B cells [C] are gated as CD19+ IgM+ CD10+ on total B cells. The CD20+ B cells are further gated [E] as memory B cells (CD19+ CD20+ CD43 dull CD27+), B1 B cells (CD19+ CD20+ CD43 bright CD27+) and naïve B cells (CD19+ CD20+ CD27 dull). Subsequently, plasmablasts (CD20 dull CD38+) are separated [D]. The naïve B cells are further gated with CD10 [F] to identify immature naïve B cells (CD19+ CD20+ CD27 dull CD10+).

Antibodies used in cocktail 2 helped in identifying various innate cell subsets. A representative image has been shown in Figure 2.

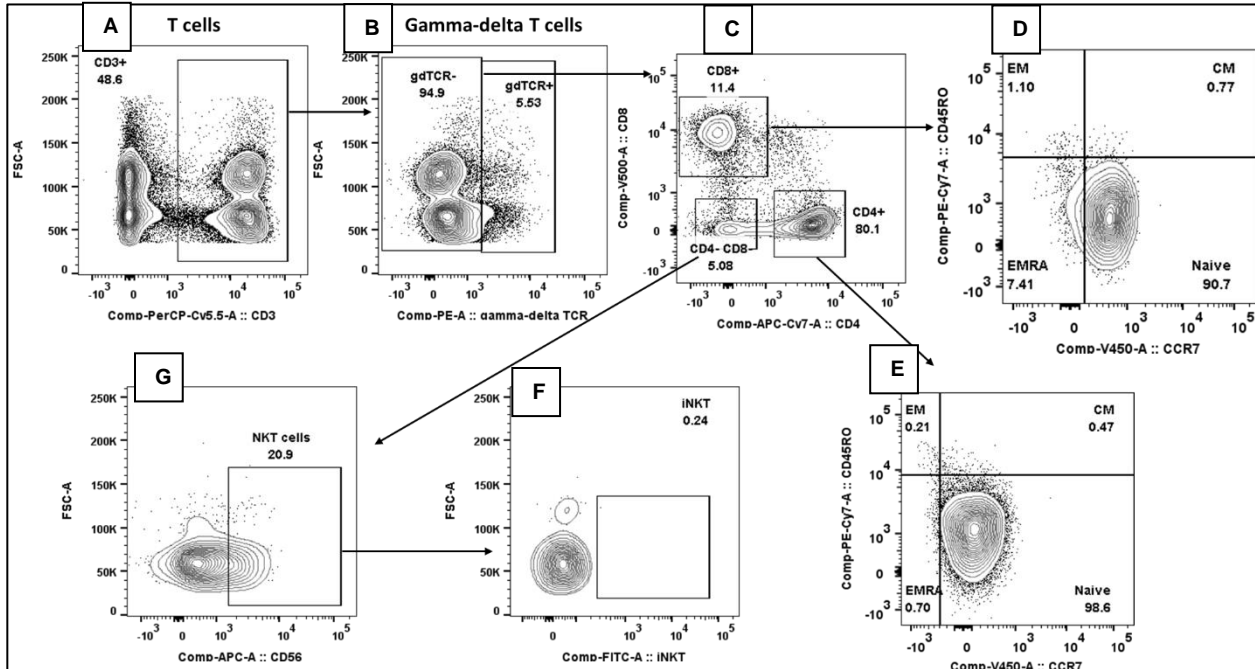
Figure 2: Flow cytometric gating strategies for innate cell subsets in cord blood.



From total leucocytes, NK cells are identified using CD56+ [A]. Dendritic cells (DCs) are separated [B] as HLA-DR bright Lineage- on total leucocytes. DCs are further classified [C] as myeloid (CD11c bright CD123 dull) and plasmacytoid (CD11c dull CD123+). From total leucocytes, Monocytes [D] are identified as CD14+ CD11c+. Subsequently, the monocytes are separated [E] as classical (CD14+ CD11c+ CD16 dull), inflammatory (CD14 bright CD11c+ CD16+), and patrolling (CD14 dull CD11c+ CD16+).

Antibodies used in cocktail 3 helped in identifying various T and NKT cell subsets. A representative image has been shown in Figure 3.

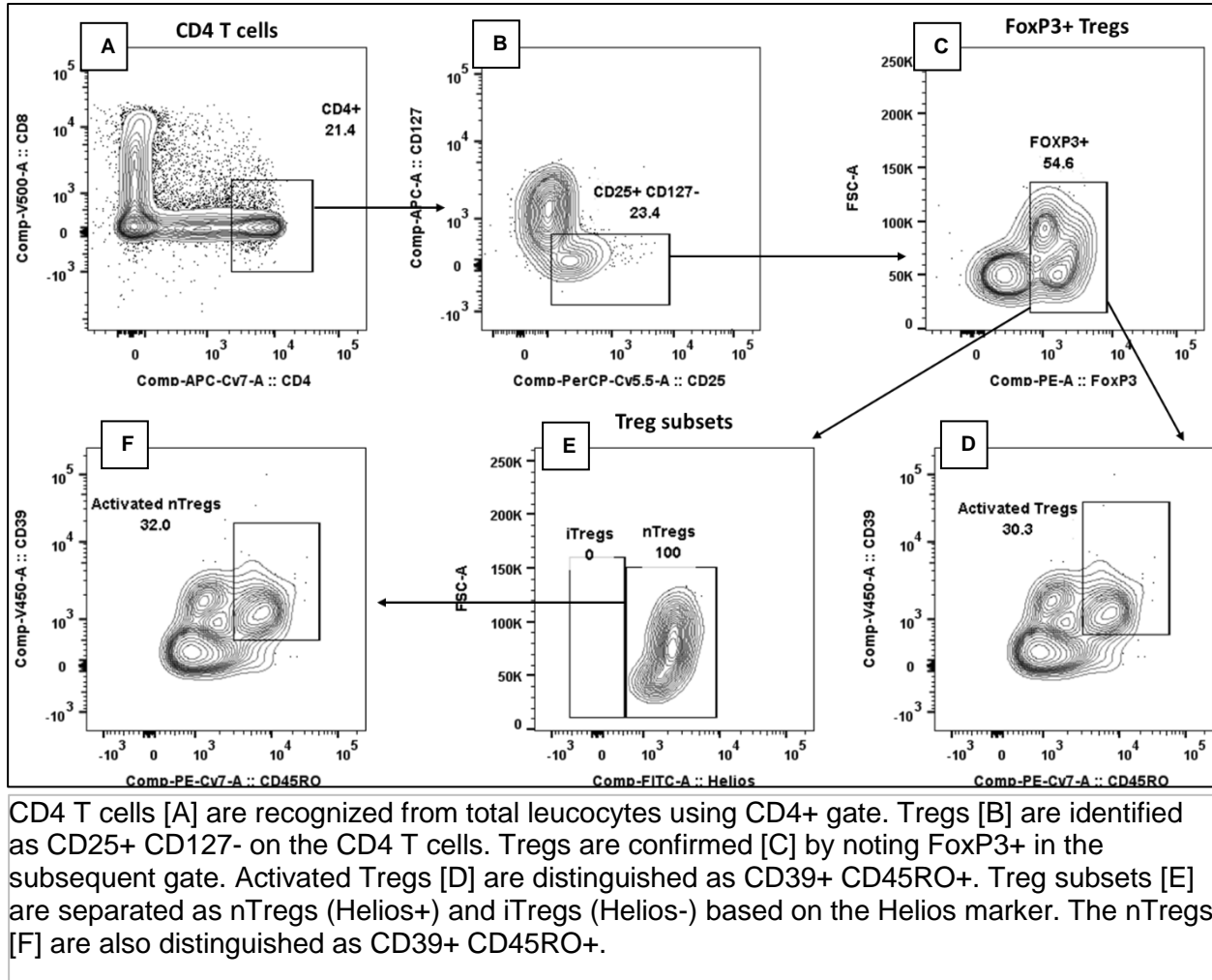
Figure 3: Flow cytometric gating strategy for T and NKT cell subsets in cord blood.



Total T cells [A] are identified as CD3+ cells in total leucocytes. $\Gamma\delta$ T-cells [B] are separated using the $\Gamma\delta$ TCR+ marker. The remaining T cells are segregated as CD4+ T cells and CD8+ T cells [C]. The CD8 [D] and CD4 [E] subsets are recognized as effector memory (CD45RO+ CCR7 dull), central memory (CD45RO+ CCR7+), EMRA (CD45RO dull CCR7-), and naïve cells (CD45RO dull CCR7+). NKT subsets [G] are distinguished as CD4- CD8- CD56+ in the $\Gamma\delta$ TCR- T cell subset. The NKT subset is further gated to isolate iNKT subset [F].

Antibodies used in cocktail 4 helped in identifying various Treg cell subsets. A representative image has been shown in Figure 4.

Figure 4: Flow cytometric gating strategy for Treg cell subsets in cord blood.



Subset Frequency Distribution Analysis:

The subset frequencies obtained via the aforementioned gating strategy were collated and plotted using Microsoft Excel and Prism GraphPad. The subsets that had an event count (actual cell numbers acquired during Flow cytometry) lower than 100 were not used for further analysis to avoid false interpretations due lack of substantial input.

These subsets are CD4 CM, CD4 EM, CD4 EMRA, CD8 CM, CD8 EM, CD8 EMRA, iNKT cells, and iTregs.

Group Analysis:

These cord blood samples were divided into three treatment groups, as per maternal nutritional supplementation: placebo, Vitamin B12 supplementation, and Vitamin B12+micronutrients supplementation. While the identity of each group will be disclosed at the end of the trial, an attempt was made to see if the patterns of various subsets differ in these groups. These groups shall be referred to as Group I, II, III. Using statistical tools such as ANOVA and Tukey's multiple comparison tests, the leucocyte subset population distributions were compared between groups to check if there were any significant differences.

Correlation Analysis:

The various leucocyte subset distributions were further analyzed to check if there existed any correlation between the percent distributions. The significant associations ($p < 0.05$) were trimmed and re-analyzed to confirm if the linear relation (positive or negative) was a result of the values at the extremities or a trend shown by the whole population.

RESULTS

Participant Population Features:

The cord blood samples collected are part of an inter-generational nutritional intervention study undertaken by Dr. Chittaranjan Yajnik from KEM Hospital, Pune. This study is based on understanding the effects of maternal nutrition on the neonatal susceptibility to cardiovascular diseases, Type 2 diabetes, and fetal growth. The present cord blood samples belong to the third generation of a population which has been carefully monitored as part of the Pune Maternal Nutrition Study (PMNS) and the Pune Rural Intervention in Young Adolescents (PRIYA) study. A total of 81 cord blood samples were received stored in liquid nitrogen.

Table 2: The participant population characteristics

<i>Neonatal Characteristics</i>	<i>Total: n=81</i>
<i>Female: n (%)</i>	<i>35 (46%)</i>
<i>Gestational age at birth (weeks)</i>	<i>Median= 39.14; Range= 28.29-41.57</i>
<i>Birth weight (kg)</i>	<i>Median= 2.695; Range= 0.925-3.6</i>

Frequency Distributions of Leucocyte Subsets:

The frequencies of all PBMC subsets were estimated as a percent of the total PBMCs (identified as shown in the gating strategy: Figure 1-4). The major proportion of PBMCs is made up of T cells (about 50-60%), followed by B cells (about 15-25%), while the monocyte, NK cell, and DC proportions are comparatively smaller (less than 15%) as seen in Figure 5. The major subsets described below were examined because they differ vastly in their functions. B and T cells are part of the adaptive immune arm. B cells on exposure differentiate to form plasmablasts that produce antibodies. T cells integrate the adaptive and innate arm by priming cells with the help of cytokines (T_H), and they also show cytotoxic abilities (T_c). Monocytes and DCs, on the other hand, are part of the innate immune arm. Monocytes are a group of heterogenous cells that carry out the function of phagocytosis (after differentiating into macrophages), cytokine production (to

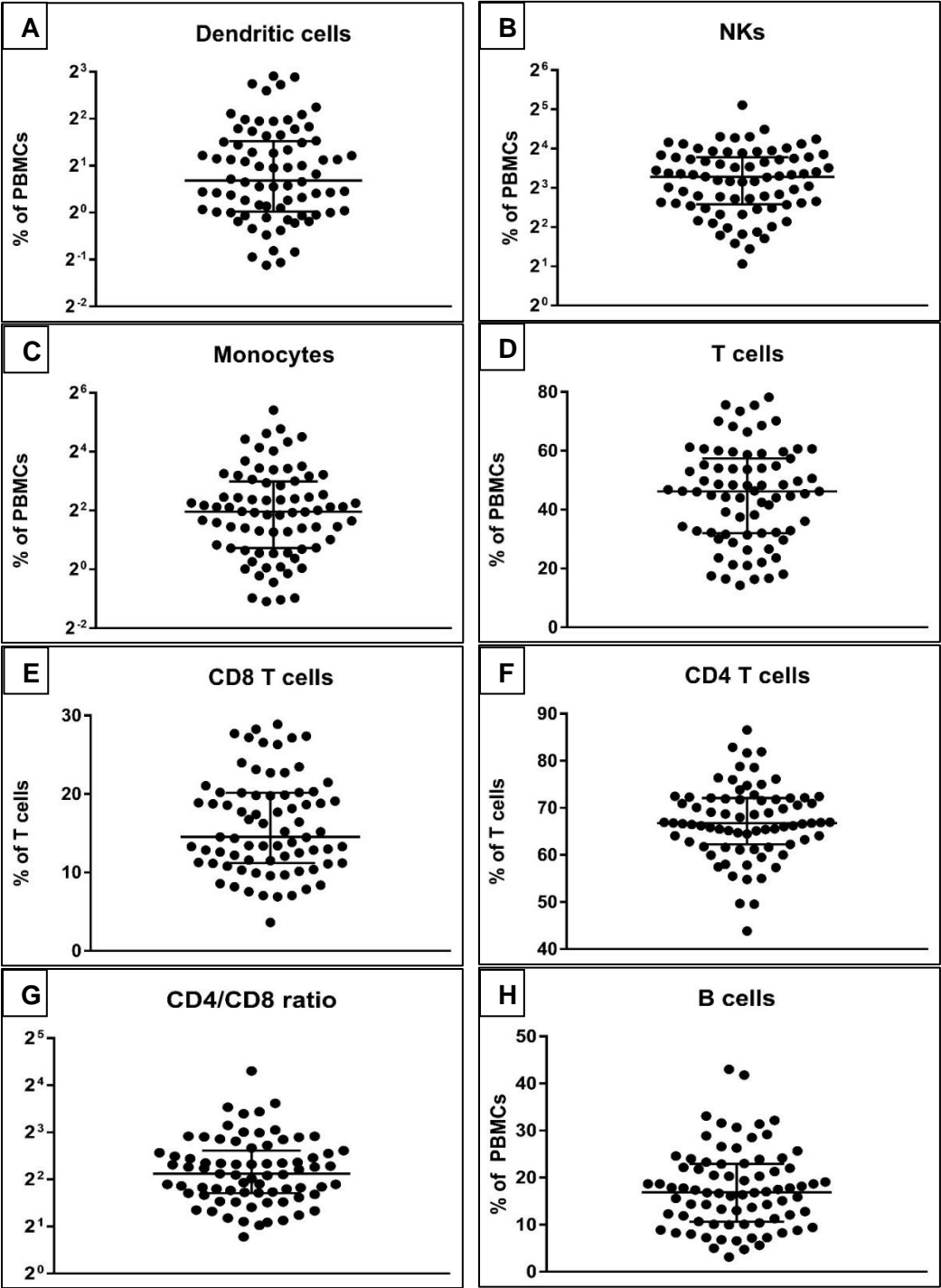
activate other immune cells) and antigen presentation (to prime the adaptive immune arm). DCs are professional antigen-presenting cells (APCs). They collect antigens at the site of the attack, process it and present it to the T cells. Conversely, regulatory T cells are immunosuppressive in nature. Moreover, CD4:CD8 ratio was used as a marker because it has been reported to have developmental significance (Amadori et al., 1995).

Table 3: Reference statistics for frequencies of immune subsets in cord blood.

Cell Subsets		25th percentile	Median	75th percentile
B cells	<i>B cells (% Total Leucocytes)</i>	10.85	16.90	22.73
	<i>B1 B cells (% B cells)</i>	0.24	0.59	1.19
	<i>Memory B cells (% B cells)</i>	0.07	0.13	0.31
	<i>Naïve B cells (% B cells)</i>	88.00	93.63	96.29
	<i>Immature B cells (% Naïve B cells)</i>	12.60	16.70	21.20
	<i>Plasmablasts (% B cells)</i>	1.04	2.04	3.32
	<i>Transitional B cells (% B cells)</i>	8.86	12.55	15.93
Monocyte, Dendritic, and Natural Killer cells	<i>Monocytes (% Total Leucocytes)</i>	1.67	3.90	7.78
	<i>Classical monocytes (% Monocytes)</i>	70.30	83.90	92.73
	<i>Inflammatory monocytes (% Monocytes)</i>	1.75	3.81	8.51
	<i>Patrolling monocytes (% Monocytes)</i>	3.30	7.39	14.85
	<i>Classical monocytes/ Patrolling monocytes ratio</i>	5.13	12.16	28.52
	<i>Dendritic cells (% Total Leucocytes)</i>	1.03	1.61	2.85

	<i>Plasmacytoid DC (% DCs)</i>	3.80	6.77	11.73
	<i>Myeloid DC (% DCs)</i>	14.15	23.70	34.50
	<i>Myeloid DC/ Plasmacytoid DC ratio</i>	1.76	3.26	6.48
	<i>Natural Killer cells (% Total Leucocytes)</i>	6.06	9.72	13.73
T cells	<i>T cells (% Total Leucocytes)</i>	32.10	46.20	56.30
	<i>CD4 T cells (% T cells)</i>	62.55	66.78	72.02
	<i>EM (% CD4 T cells)</i>	0.71	1.19	1.65
	<i>CM (% CD4 T cells)</i>	0.20	0.40	0.54
	<i>EMRA (% CD4 T cells)</i>	0.78	1.50	3.50
	<i>Naïve (% CD4 T cells)</i>	94.10	96.90	97.75
	<i>CD8 T cells (% T cells)</i>	11.25	14.54	20.03
	<i>EM (% CD8 T cells)</i>	0.29	0.63	1.17
	<i>CM (% CD8 T cells)</i>	0.63	1.20	2.42
	<i>EMRA (% CD8 T cells)</i>	7.96	12.90	23.10
	<i>Naïve (% CD8 T cells)</i>	74.35	84.50	89.80
	<i>CD4/CD8 ratio</i>	3.28	4.36	6.03
	<i>Gamma-delta T cells (% T cells)</i>	6.01	8.13	11.90
	<i>NKT cells (% T cells)</i>	0.24	0.61	1.42
<i>iNKT cells (% T cells)</i>	0.00	0.00	0.19	
Tregs	<i>Tregs (% CD4 T cells)</i>	3.86	5.60	7.21
	<i>Activated Tregs (% of Tregs)</i>	10.90	18.00	28.40
	<i>nTregs (% of Tregs)</i>	99.30	99.80	100.00
	<i>iTregs (% of Tregs)</i>	0.00	0.19	0.66
	<i>Activated nTregs (% of nTregs)</i>	14.70	27.60	39.70

Figure 5: Major subset frequency distributions.

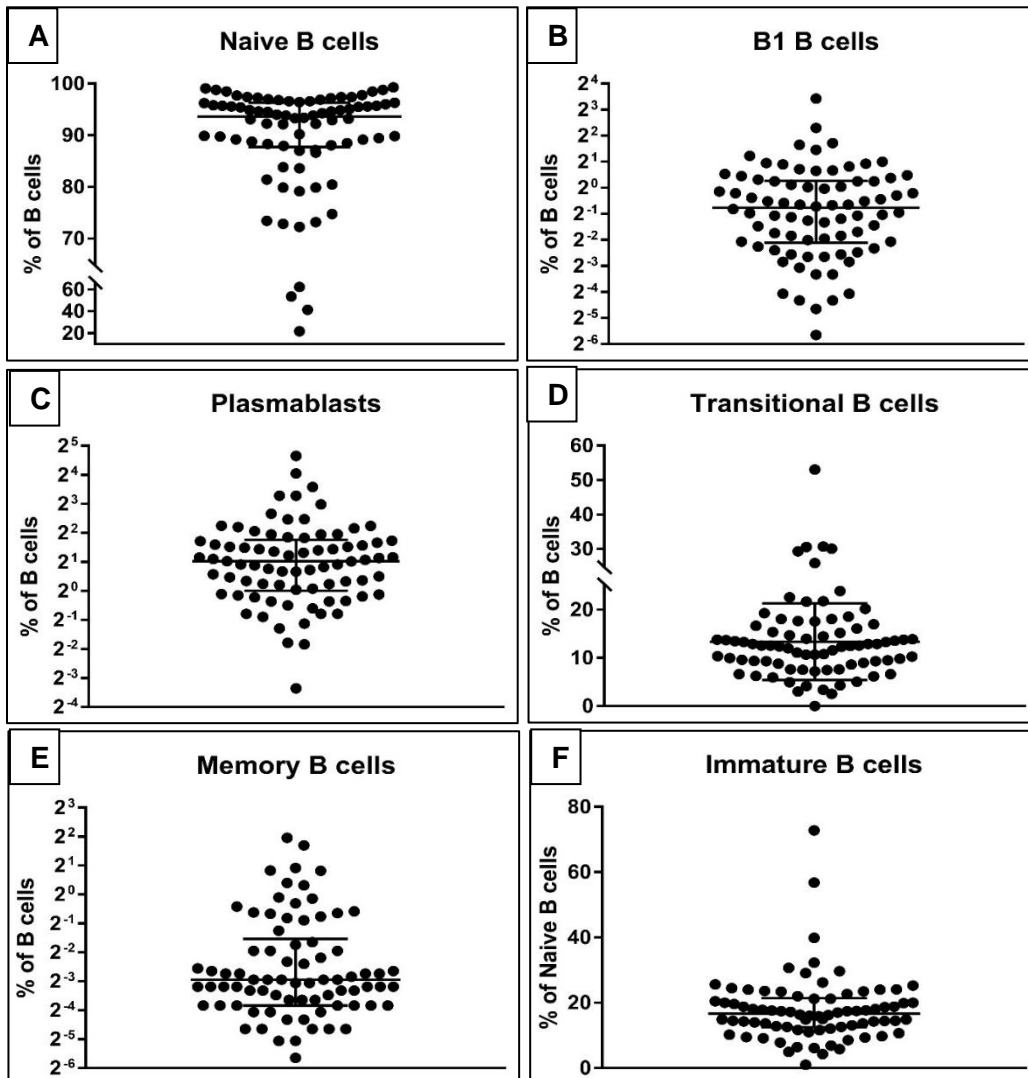


As indicated, Dendritic cell [A], Natural Killer cell [B], Monocyte [C], T cell [D], and B cell [H] frequencies are expressed as percent of PBMCs. The CD8 T cell [E] and CD4 T cell [E] frequencies are expressed as percent of T cells, and the CD4/CD8 ratios [G] are shown here. The data is represented with the median and interquartile range. Each dot represents values from individual cord blood sample.

Frequency distribution of B, T, NKT, Tregs, monocyte and dendritic cell subsets:

The B cell subsets that have been segregated are naïve B cells, B1 B cells, immature naïve B cells, transitional B cells, Plasmablasts and memory B cells. The most predominant subset as seen in Figure 6, is that of naïve B cells.

Figure 6: B cell subset frequency distributions.



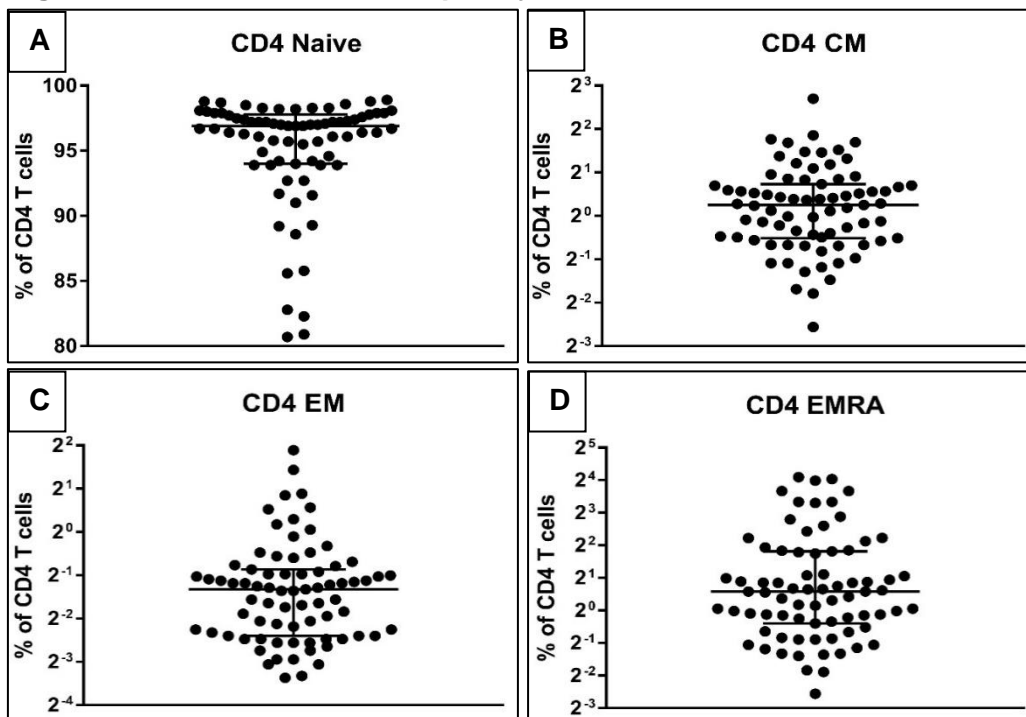
All subset [A-E] frequencies are expressed as a percent of B cells. The immature B cell [F] frequencies are expressed as a percent of naïve B cells. The data is represented with the median and interquartile range. Each dot represents values from individual cord blood sample.

About 15-20% of these naïve cells are immature naïve cells recognized by the presence of CD10 on their cell surfaces. A significant yet comparatively smaller proportion of B

cells is constituted by transitional B cells. Transitional B cells range from 10-20%, while only rare individuals show starkly higher frequencies ranging from 25-50%. The B1 B cells frequency ranges from 0.2-8%, showing an immense amount of variability within the population. A surprising observation made as part of this analysis was the seemingly high proportions of plasmablasts in some neonatal samples, ranging from 0.25% to 16%. The frequencies of memory B cell for the majority of the population was lower than 1%; however, even in this case, there were some individuals that showed higher frequencies of up to 4%.

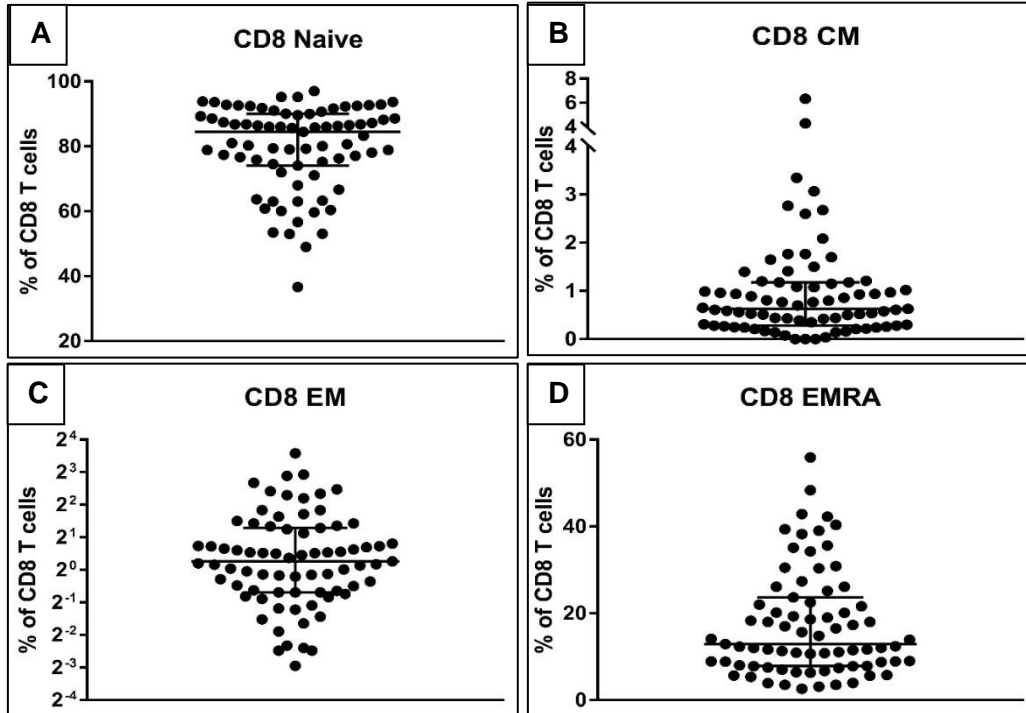
The CD4 and CD8 T cell subsets comprise of naïve, central memory, effector memory, and effector memory recently activated cells as seen in Figure 7 and 8. About 80-100% of the CD4 and CD8 T cells are naïve CD4 and CD8 T cells. The CD4 memory cells range from 0.1-8%, while there is a considerably higher proportion of CD8 memory cells. However, since the actual cell count (number of events within the gate) for all these memory subsets was less than 100, no further analysis was done to determine if these were real trends, due to lack of robust data.

Figure 7: CD4 T cell subset frequency distributions.



The subset [A-D] frequencies are expressed as a percent of CD4 T cells. The data is represented with median and interquartile range. Each dot represents values from individual cord blood sample.

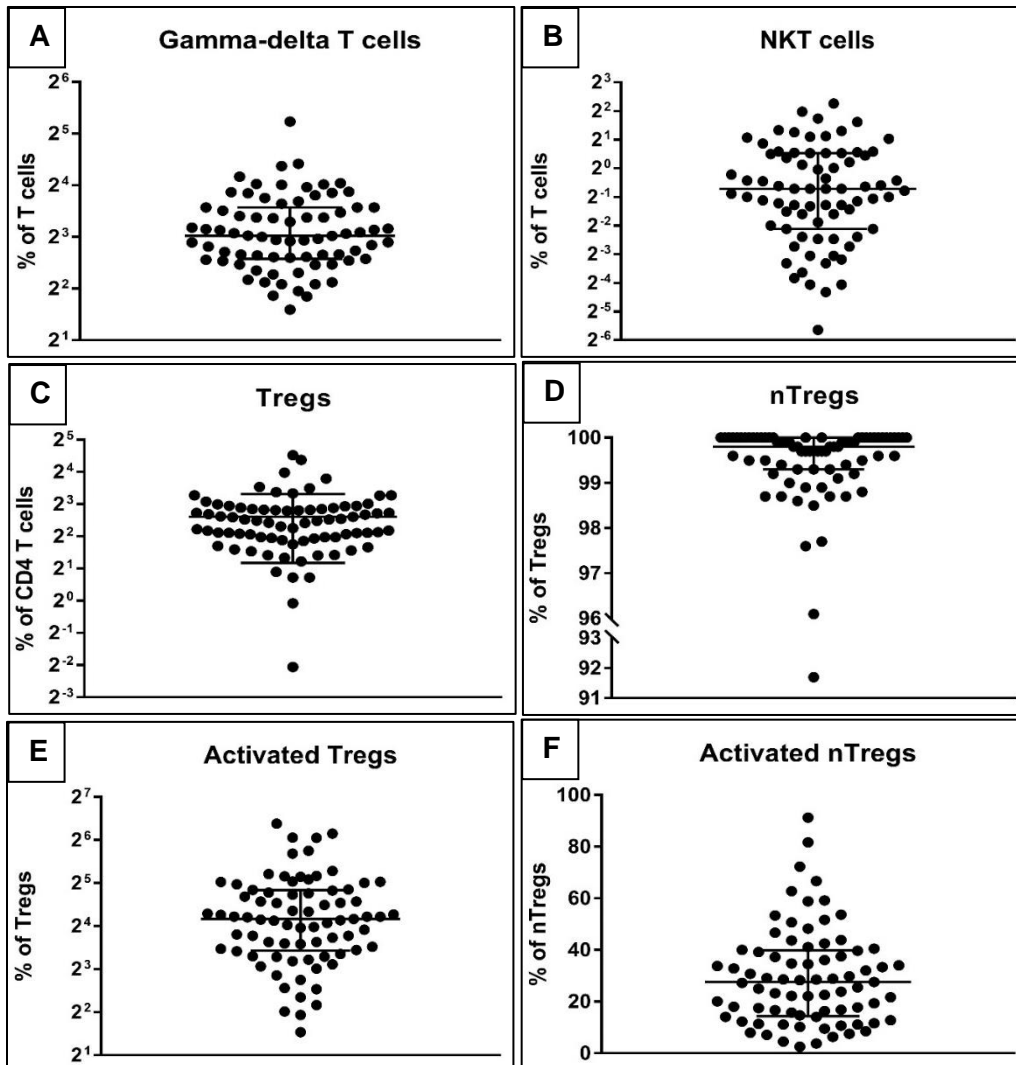
Figure 8: CD8 T cell subset frequency distributions.



The subset [A-D] frequencies are expressed as a percent of CD8 T cells. The data is represented with the median and interquartile range. Each dot represents values from individual cord blood sample.

The other T cell subsets that were analyzed were gamma-delta T cells, NKT cells and regulatory T cells (Tregs) as shown in Figure 9. The gamma delta T cells frequencies showed a spread between 4-16% of total T cells. The NKT cell frequencies were ranging between 0.1-4% of total T cells. These subset populations are comparatively rarer than CD4 or CD8 T cells as expected. The last T cell subset, Tregs comprised of 2-16% of the CD4 T cells. Of these Tregs, about 99% were nTregs, as expected and 0-1% were iTregs. However, since the actual cell counts for iTregs were less than 100, this subset was not studied further. Surprisingly, there was a substantial proportion of about 8-32% of activated Tregs.

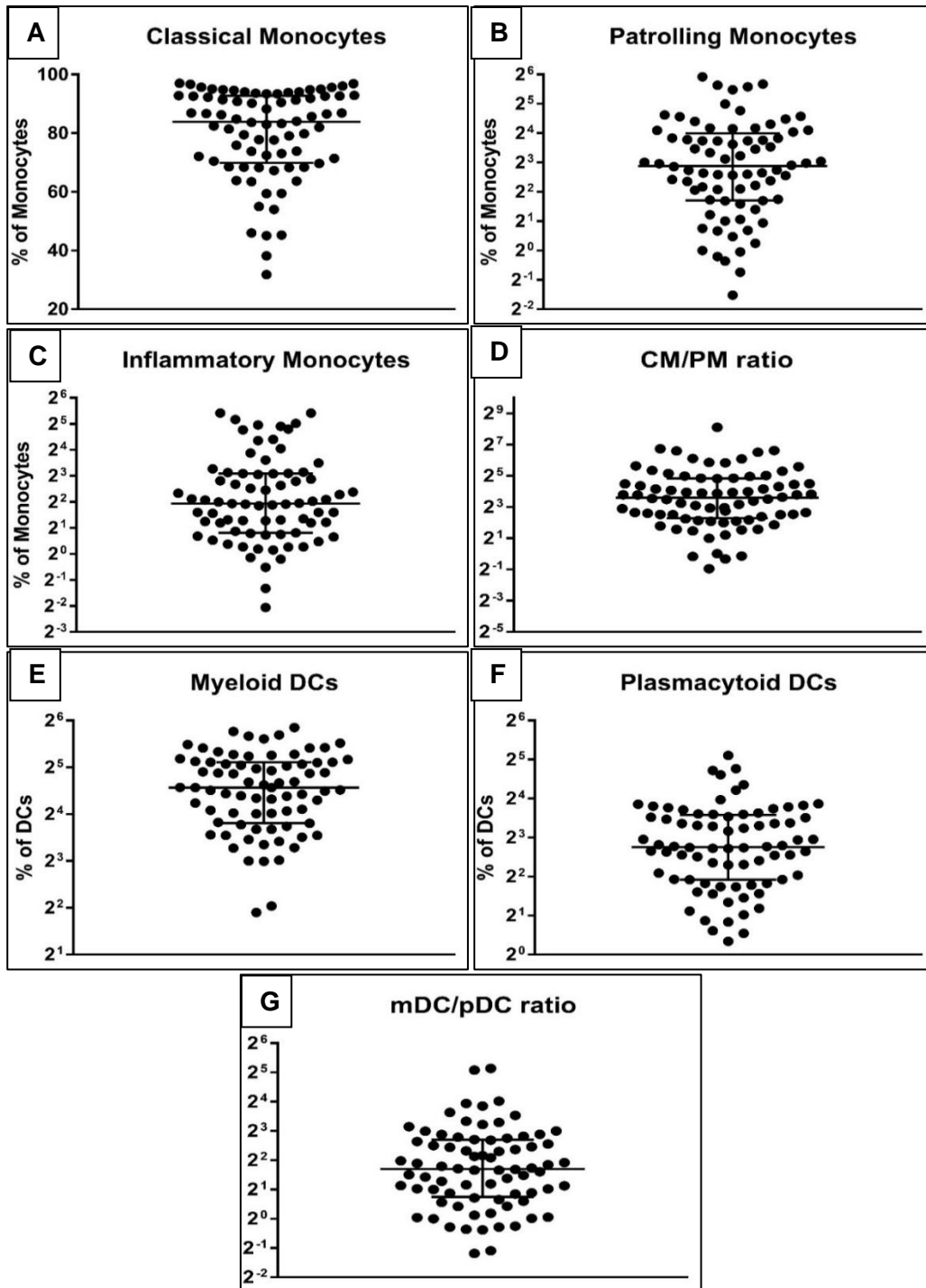
Figure 9: T cell subset frequency distributions.



The frequencies of gamma-delta T cells [A] and NKT cells [B] are expressed as a percent of T cells. Treg frequencies are expressed as a percent of CD4 T cells. Activated Treg and nTreg frequencies are expressed as a percent of Tregs and activated nTregs frequencies are expressed as a percent of nTregs. The data is represented with the median and interquartile range. Each dot represents values from individual cord blood sample.

The last subsets analyzed were monocytes and dendritic cell populations as depicted in Figure 10. While 80-100% of the total monocytes were classical monocytes and 4-16% were patrolling monocytes, the inflammatory monocytes made up a comparatively small proportion of 2-10% of total monocytes. The plasmacytoid dendritic cell subsets and myeloid dendritic cell subsets made up 4-16% and 8-32% of the total DCs respectively.

Figure 10: Monocyte and DC subset frequency distributions.



The subset [A-C] frequencies are expressed as a percent of monocytes, and the subset [E-F] frequencies are expressed as a percent of DCs. The classical monocytes: patrolling monocytes ratio is depicted in [D] and the myeloid DC: plasmacytoid DC ratio is shown in [G]. The data is represented with the median and interquartile range. Each dot represents values from individual cord blood sample.

The other DC subsets could not be identified since only CD123, and CD11c were used

as markers during staining.

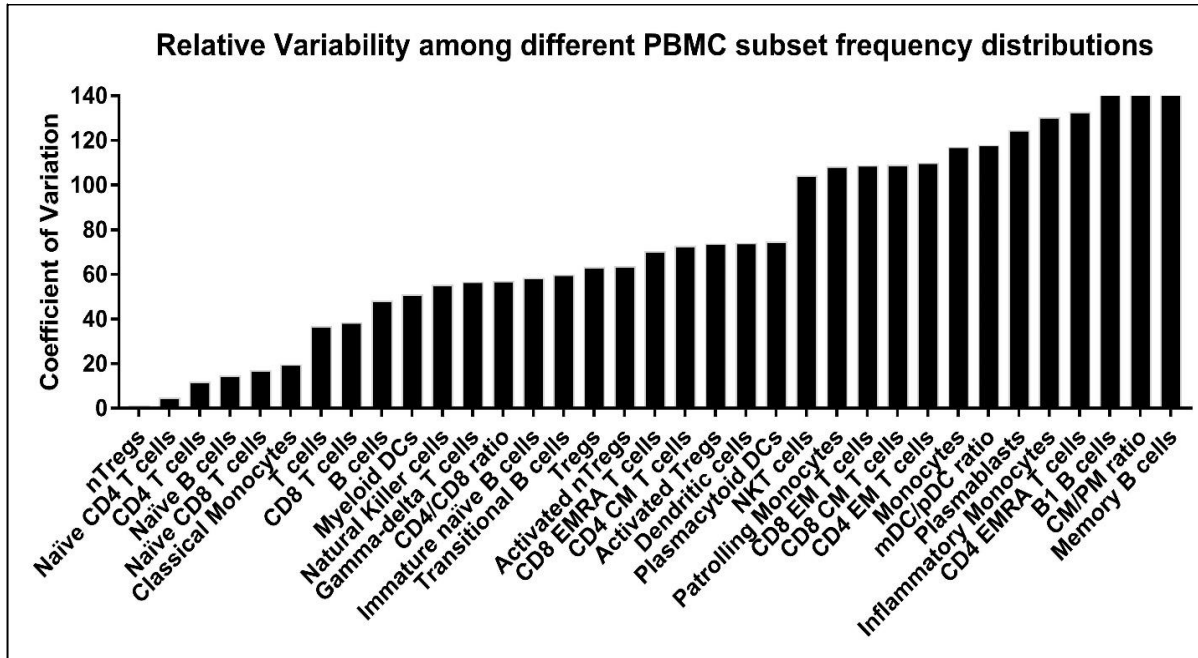
Although highly variable, the mDC/pDC ratio averaged at 4, and the CM/PM ratio had a mean of about 16. The frequencies of these cell subsets show a tremendous amount of variability within the population.

Mean normalized standard deviation of PBMC subsets showed enormous variation:

The coefficient of variation (CV) for each subset was calculated as

$$\text{Coefficient of variation} = \frac{\text{Standard deviation of subset frequency}}{\text{Mean of subset frequency}} \times 100$$

Figure 11: Coefficient of variation of immune subset frequencies in cord blood.



Values on the y-axis show the coefficient of variation calculated as indicated above. The x-axis shows the various immune subsets being analyzed.

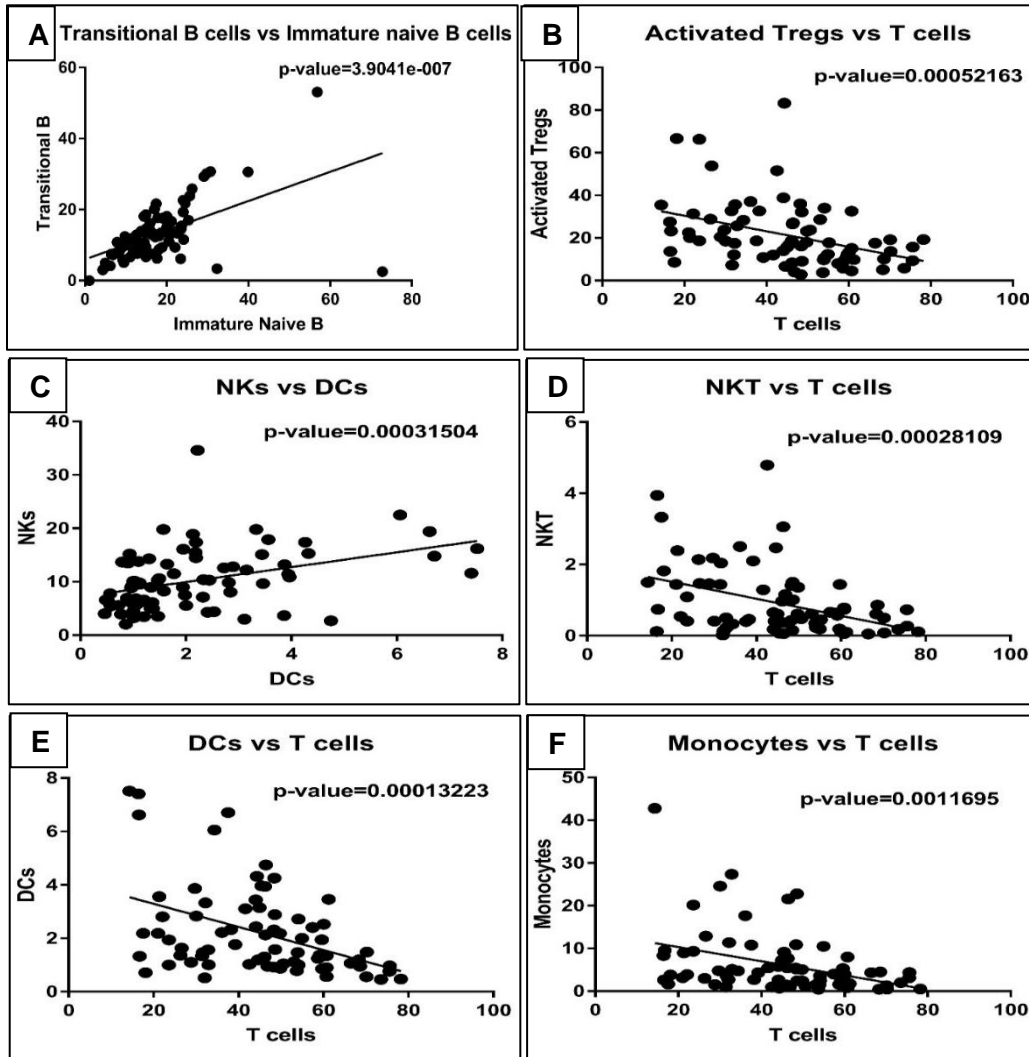
The coefficient of variance signifies a normalized dimensionless parameter used to compare quantities with starkly different units of measurement. The variability in the CVs ranges from 5-140% of the mean. Hence, it must be noted that the spread of the relative frequencies of each subset shows a great deal of variation. As seen from Figure 11, nTregs, naïve CD4 and CD8 T cells, naïve B cells, CD4 and CD8 T cells, T cells and classical monocytes show a comparatively lower relative variability in the range of

5-20% of the mean, while plasmablasts, memory B cells, B1 B cells, CD4 EMRA T cells, and inflammatory monocytes show a much higher amount of variability in the range of 120-140% of the mean.

Some PBMC subsets show significant correlations:

Transitional B cells show tight correlations with immature naïve B cells. As seen in Figure 12, A: The relative frequency of transitional B cells increases proportionately with immature naïve B cell frequencies. Additionally, another positive correlation is seen between NK cells and DCs. Here NK cell frequencies are increasing with a much steeper slope with an increase in DC frequencies.

Figure 12: Correlations between cord blood immune subset frequencies.



The p-values are indicated in each individual panel [A-F]. The best fit trendline has been inserted. Each dot represents values from individual cord blood sample.

Next, T cell frequencies show a negative correlation with a number of subsets such as activated Tregs, NKTs, monocytes, DCs. Here, as the relative frequency of T cells increase, the corresponding subset's relative frequencies drop significantly. The correlations that arise as a result of the gating strategy used have been eliminated. The ones elaborated on here are significant and non-spurious in nature.

No statistically significant differences were observed in the immune subset frequency distributions of the three test groups:

As described earlier, the entire test population was subdivided into three treatment groups: Group I, II, and III. No significant difference in means was observed in any of the subset frequencies between the groups within a 95% confidence interval. For all immune cell subsets, the Brown-Forsythe test indicated comparable variances. Furthermore, multiple comparisons such as I vs. II, II vs. III and I vs. III reported no significant differences in the mean frequencies (Data not shown here).

DISCUSSION

As part of this cross-sectional interventional study, a large number of immune cell lineages and sub-lineages have been immunophenotyped in detail for 81 cord blood samples. These data will provide statistics on cord blood immune cell frequencies from 6 villages around Pune, thus establishing a standard for this ethno-geographical and socio-economical population. Since this cohort has been monitored for over three generations as part of the ongoing PMNS and PRIYA studies, it has generated a lot of data not only highlighting the role of maternal nutrition in fetal programming (Yajnik et al., 2008) but also to study the variation observed in a population belonging to the same socio-economic background and ethno-geographical group.

Sample collection has been continuing and until that ends the actual treatment received by the mothers in the three groups will not be disclosed. Hence, interim analysis has been carried out to look for obvious major differences in the three groups, if any. At this stage, the immunophenotyped data doesn't show any significant differences between the three treatment groups, namely; placebo, Vitamin B12 supplementation, Vitamin B12 and micronutrient supplementation; in terms of the immune subset frequencies. However, some interesting trends have been observed in the immune sub-lineages within this population. Since these are cord blood samples, the variation seen within the frequencies of each subset can be primarily attributed to genetic variation, as the neonate is expected to develop in an immunologically sterile environment. However, this being said the data shows some individuals to have a significant percentage of plasmablasts which means that these neonates have encountered foreign antigens. Moreover, it is also surprising that there was no correlation observed between increasing plasmablast frequencies and memory B cells if at all the neonate had been exposed to pathogens.

As expected, the highest frequencies of immune sub-lineages observed are that of naïve B cells, naïve CD4 and CD8 T cells. Also, the high CD4/CD8 ratios with a median between 2-4 observed in cord blood are in agreement with data shown from another cross-sectional study in Delhi (Prabhu et al., 2016).

Regulatory T cells (Tregs) are broadly divided into two subgroups: natural Tregs (nTregs) and induced Tregs (iTregs). nTregs are generated in the thymus from T cell precursors and are committed to the Treg phenotype. iTregs, on the other hand, are generated from naïve T cells on stimulation in the periphery in the presence of TGF- β and IL-2. These iTregs take over the immunosuppressive roles of nTregs as and when their response turns anergic or defective (Fontenot et al., 2003; Chen et al., 2003). Moreover, iTregs generate antigen-specific suppression in immune responses and in neonates, there is possibly no ongoing in-utero immune assault, thus explaining their absence/ very low frequencies.

Monocytes are broadly divided into three subsets: classical, inflammatory and patrolling. Classical monocytes (CM) majorly carry out phagocytic activities while producing basal levels of pro-inflammatory cytokines. Inflammatory monocytes (IM) as the name suggests actively produce pro-inflammatory cytokines like IL-1 β , IL-6, and TNF- α . Patrolling monocytes (PM) are anti-inflammatory in nature and produce IL-1RA predominantly. In the present cord blood samples, CMs make up the majority of the population as expected. IMs show similar percentages to data shown from another population study in Delhi (Prabhu et al., 2016). PMs on the other hand show elevated percentages than that reported in the Prabhu et al. study. A possible explanation could be that raised PM percentages are related to immune exposures seen in some babies of this population as described above in the context of plasmablast percentages.

The coefficient of variation plotted for each immune sub-lineage highlighted a noteworthy trend. There were some lineages like nTregs, naïve CD4 and CD8 T cells, naïve B cells, CD4 and CD8 T cells, T cells and classical monocytes that showed very limited variation as compared to the mean (about 5-20%), suggesting that these subset frequencies are genetically more tightly regulated than the others. Conversely, there were some lineages such as plasmablasts, memory B cells, B1 B cells, CD4 EMRA T cells, and inflammatory monocytes, that showed an immense amount of variation up to 140% of the mean frequency. A probable reason for this could be the developmental differences in temporal terms since some of the babies in this study are premature with low birth weight.

Furthermore, the inter-subset correlations that arose out of this study highlighted a possibility of establishing relationships between “apparently” unrelated subsets, since their relative frequencies showed a significant positive or negative correlation. There was a tight positive correlation between transitional B cells and immature naïve B cells. In the developmental pathway, transitional B cells form an intermediate between immature B cells and mature naïve B cells. Intuitively (as shown in Figure 12, A) as the immature naïve B cell frequencies rise, there is a parallel increase in transitional B cell frequencies. Moreover, in order to identify whether these subsets are actually distinct sub-populations of B cells, we need to look at differentiating markers such as CD5, CD43 and IgD (Sims et al., 2005; Agarwal and Smith et al., 2013).

Another significant positive correlation is seen between NK cells and DCs (as shown in Figure 12, C). The trend as seen demonstrates that relative prominence of both these subsets increases. This could either mean that their actual cell numbers linked or that another population is vastly varying altering the total PBMC numbers as a result of which their respective niches could be interlinked. Either way, there seems to exist a quantitative linkage. NK cells are from the lymphoid lineage and most cord blood DCs are from the myeloid lineage (Lee et al., 2015). This suggests that there may exist common signaling factors that positively regulate both myeloid and lymphoid lineages.

The data shows a negative association between activated Treg and T cell frequencies (as shown in Figure 12, B). Also, there is no significant correlation between T cells and Treg percentages. Therefore, probably there is an apparent link between the ‘activated’ phenotype and T cell numbers. One probable explanation could be that when T cell numbers are high, (since T cells and Tregs get primed in the secondary lymphoid organs) the probability of Tregs encountering antigens dramatically decreases because of the space constraint in lymph nodes.

Furthermore, a negative correlation can be seen between NKT cells and T cells (as shown in Figure 12, D). NKT cells form a subset of T cells, thus there could be a relative increase in the other T cell subsets such as $\gamma\delta$ T cells, CD4 T and CD8 T cells, which emerges as an effective decrease in NKT cells, which appears to be significant because NKT cell frequencies are primarily very low (1-3%).

Lastly, there exists a negative correlation between T cell frequencies and DC/monocyte frequencies as shown in Figure 12, E and F). Like in the case of NKs and DCs correlation, the probable link is that of a common signaling factor that connects the myeloid and lymphoid lineage regulations. In this case, however, the factor has an inhibitory effect on the myeloid lineage (as DC and monocyte relative frequencies decrease) and a stimulatory effect on the lymphoid lineage (as T cell frequencies go up). This effectively translates in DC and monocyte prominence being negatively associated with T cell prominence.

Therefore, this interim analysis has provided us with valuable insights on the inherent variations within the immune system of this population, while highlighting some meaningful correlations which could generate useful data on further analysis.

Part II: Effect of Temperature on T cell differentiation

INTRODUCTION

Fever initiation: Common to endotherms and ectotherms

Raised body temperatures have been considered one of the four chief indicators of inflammation and is produced in response to an immune challenge by pathogens. It is characterized by a rise in body temperatures typically by 1-4°C. This fever response is seen in all vertebrates, both endotherms, and ectotherms. Despite having completely different thermic strategies, and fever production being a costly response since 10-12.5% extra energy needs to be expended to raise the temperature by 1°C, on the whole, the cost-benefit ratios incline in favour of raised body temperatures. Moreover, since fever is a whole-body systemic response, it affects the innate as well as the adaptive immune arms (Evans et al., 2015).

Current research has been focused on trying to understand the role of fever in immune responses to pathogens, by attempting to decipher the molecular networks involved and the key players in this complex cascade. Also, it is important to trace this effect from the sensory pathways that detect variations in temperature to the downstream events that trigger amplified immune responses. Thus, this is a very important and dynamic study.

Fever boosts the innate immune arm

The innate immune arm plays the role of a “first responder.” Some of the important innate immune cells that are positively affected by whole-body hyperthermia include neutrophils and natural killer (NK) cells. These cells respond to foreign antigen stimulation via bacteriolytic and cytotoxic activities. Furthermore, a “burst” of leukocytes from the bone marrow is induced in response to a rise in body temperature. This results in an increased number of neutrophils in circulation, allowing for better recruitment to local inflammatory sites with the aid of cytokines like IL-1 β , TNF- α , which are also endogenous pyrogens (Tulapurkar et al., 2012; Jiang et al., 1999).

Moreover, the febrile response also upregulates toll-like receptors (TLRs) expression on the cell surface which is compounded with an enhanced phagocytic ability of macrophages and dendritic cells. An in vitro study revealed that heat treatment

produced a two-fold increase in L-selectin-like adhesion and rolling of leukocytes to the endothelial membrane. This enhanced adhesion translates directly into the better recruitment of cells to inflammatory sites (Appenheimer et al., 2007).

Another study demonstrated that high temperatures downregulated MHC Class I expression and enhanced HSP70 (Heat shock protein-70) formation in vivo, both of which are associated with enhanced cytotoxic abilities and recruitment of NK cells to tumor sites (Kappel et al., 1991; Burd et al., 1998; Multhoff et al., 1995). Hyperthermia also augments the ability of antigen presenting cells (APCs) to assist the adaptive immune arm. A mice study showed that the maturation of skin dendritic cells (Langerhans cells) was boosted by fever which allowed their faster migration to lymph nodes for antigen presentation to the naïve lymphocytes and initiation of an adaptive response (Basu et al., 2003).

Fever and T cell responses

T lymphocytes play a crucial role in adaptive immune response generation. On primary exposure, naïve CD4 T cells get stimulated and differentiate into effector CD4 T cells depending upon the stimulation cue and microenvironment. During this differentiation process, epigenetic reprogramming of the cell takes place which polarizes its lineage fate to either a Th1, Th2, Th17, Tregs, or Tfh phenotype (Zhu et al., 2010)

The febrile response has been reported to intensify T cell stimulation and differentiation to produce a faster, more robust reaction. A mice study revealed that whole body hyperthermia induces a surge in circulating T lymphocytes in tissues. Furthermore, this study also showed these T cells to possess polarized cytoskeletal spectrins, uropods and increased protein kinase C (PKC) activity suggesting that thermal stress can regulate essential signal transduction pathways for activation and differentiation (Wang et al., 1999). Another report demonstrated beneficial effects of fever-range temperatures on lymphocyte homing to lymph nodes and spleen within about 4 hours in an L-selectin and $\alpha 4\beta 7$ -integrin-dependent manner. This altered response affected the interaction of these lymphocytes with high endothelial venules (HEVs). Moreover, it was noted that the adhesion receptors on lymphocytes and ligands on HEVs were bimodally

modulated, indicating direct evidence connecting thermal stress with improved immune surveillance post infection (Evans et al., 2001; Wang et al., 1998).

These findings highlight the role of fever as an immune amplifier. Therefore, there is a need to understand the exact molecular pathways via which T cells sense temperature changes and alter their effector responses.

Temperature sensing mechanisms in T cells

For any downstream response to be produced, T cells first need to sense temperature fluctuations. There could be multiple, degenerate, alternative or synergistic pathways for temperature sensing in T cells.

From recent studies, one such pathway that has emerged is via alterations in the fluidity of the phospholipid bilayer. Temperature modulations manifest as changes in membrane fluidity depending on the phospholipid composition of the membrane. Both *in vitro* and *in vivo* studies have shown that hyperthermia enhances CD microdomain clustering and reorganizes cytoskeletal elements by directly altering membrane fluidity. Both these effects play a vital role in T cell stimulation. Furthermore, in CD4 T cells, it has been demonstrated that mild hyperthermia acts as a surrogate for CD28 co-stimulation and enhances IL-2 production. Parallely, in CD8 T cells the naïve to effector transition has been shown to be temperature sensitive, and at high temperatures, there is an increased IFN- γ production which enhances the formation of immunological synapses. These results suggest that temperature plays a role in lowering T cell activation thresholds. However, the exact downstream cascade at play has not been identified (Zynda et al., 2015; Mace et al., 2011).

Another proposed mechanism for temperature sensing in T cells is via temperature-sensitive transient receptor potential (TRPs) channels, in particular, TRPV1 which has shown to be expressed in CD4 T cell plasma membranes. A mouse study recently showed that TCR stimulation and cytokine production is significantly reduced in TRPV1 knockout mice. This highlights an emerging role of TRPs as thermosensitive TCR-stimulating channels (Bertin et al., 2014; Majhi et al., 2015).

In the current study, efforts have been made to understand the role of fever in T cell effector fate (Th1 vs. Th2) decisions, which are governed by the transcription factors Tbet and Gata3 and understand whether fever directs differentiation preferentially towards one fate relative to the other.

MATERIALS AND METHODS

The cell line used: Human T lymphocyte cell line, Jurkat (Clone E6-1; ATCC TIB-152) was used for all the experiments involving studying effects of temperature on T cell response. This is a pseudodiploid human cell line derived from a 14-year-old male. This cell line originates from an acute T cell leukemia and is morphologically a lymphoblast.

Jurkat Culture and maintenance: The human T cell line, Jurkat is grown at 37°C in RPMI 1640 (PAN BioTech: Catalogue no- P04-22100) with additional 10% FBS (Thermo Fisher Scientific: Catalogue no- 16000-044), 1% Antibiotic-Antimycotic solution (Sigma: Catalogue no- A5955): 100U/ml Penicillin, 100µg/ml Streptomycin and 0.25 µg/ml amphotericin B; and 2mM L-Glutamine (Sigma: Catalogue no- G7513). During every subculture, 0.1million cells/ml are seeded in fresh medium. The cells are sub-cultured when the flask reached 70-80% confluency.

Jurkat Activation: Jurkat cells are activated with CD3 and CD28 antibodies. The well plates are first incubated at 37°C for 60 minutes with the antibodies CD3 (5µg/ml) and CD28 (1µg/ml) in 1x PBS. The antibodies adhere to the well plate surface. Next, the excess antibodies are washed off, and appropriate density of Jurkat cells are seeded into these treated wells.

Primer Design and Validation: Primers for the following transcription factors were designed using Spleign and Primer3Plus online tools: Gata3, Tbet, ROR-γ, Stat6, Gfi-1, cMaf, FoxP3 and 18s rRNA. The primers were then BLASTed using Primer-BLAST to ensure that all gene isoforms are recognized.

Primer sequences for human transcription factors designed are as follows:

➤ Gata3: Amplicon size- 130bp

Forward: 5'-AACTGTCAGACCACCACAACCACAC-3'

Reverse: 5'-GGATGCCTTCCTTCTTCATAGTCAGG-3'

➤ T-bet: Amplicon size- 111bp

Forward: 5'-GTGACTGCCTACCAGAATGCC-3'

Reverse: 5'-GCTGGTGTCAACAGATGTGTA-3'

➤ ROR-γ: Amplicon size- 181bp

Forward: 5'-CAGAGCGTCTGCAAGTCCTA-3'

Reverse: 5'-CGAACTCCACCACGTAAGTGA-3'

➤ Stat6: Amplicon size- 176bp

Forward: 5'-GGAAGGGCACTGAGTCTGTC-3'

Reverse: 5'-GGCATTGTCCCACAGGATAG-3'

➤ Gfi-1: Amplicon size- 160bp

Forward: 5'-ACAGCGGTACCAGACCCTTT-3'

Reverse: 5'-AGGTGTGTGGACAGTGTGGA-3'

➤ cMaf: Amplicon size- 173bp

Forward: 5'-CCAGGACTTCGCTATTTTGC-3'

Reverse: 5'-TCCTCTTCTGCTTGGCTCTC-3'

➤ FoxP3: Amplicon size- 173bp

Forward: 5'-CAGAGCTCCTACCCACTGCT-3'

Reverse: 5'-TGCTGCTCCAGAGACTGTACC-3'

➤ 18s rRNA: Amplicon size- 101bp

Forward: 5'-CGCCGCTAGAGGTGAAATTCT-3'

Reverse: 5'-CGAACCTCCGACTTTCGTTCT-3'

All primers, custom synthesized from Sigma were PCR amplified using cDNA synthesized from Jurkat cells and analyzed on an agarose gel for expression. Each primer pair has a different annealing temperature (55-65°C), and optimum temperature was determined.

Since 18s rRNA is constitutively active, it was used as a positive control for all experiments. For testing effects on Jurkat cells incubated at 37°C and 40°C RT-PCR analysis was carried out only on transcription factors GATA3 and Tbet.

RT-PCR: Cells were incubated for 6h, 16h, and 24h with/without CD3/28 stimulation at either 37 or 40°C. Harvested cells were stored at -80°C in TRIzol reagent (Thermo-Fischer Scientific: Catalogue no- 15596026). The cells were also counted (using Trypan

Blue staining) and viability was calculated before freezing. On an average, viability was in the range of 80-95%.

RNA was extracted by the TRIzol-Choloform method, and isopropanol-ethanol was used to precipitate the RNA. The RNA was quantified on the NanoDrop2000 using spectrophotometry (nucleic acids have an absorbance at 260nm). The average 260/280 ratio was ~1.8.

For cDNA synthesis, 500ng of input RNA was used along with the Verso cDNA synthesis kit (Thermo Fisher Scientific: Catalogue no- AB1453A). The cDNA quality was evaluated by doing PCR with constitutively expressed 18s rRNA primers.

RT-PCR was performed using Pfu enzyme (A gift from Dr. Gayathri Pananghat) and 10x Pfu buffer (100mM Tris-HCl, 20mM MgCl₂, 500mM KCl; buffer pH 8.3 at 25°C) for both GATA3 and Tbet. The PCR set up had 20ng of the enzyme in 20µl final volume. The reaction mixture also contained 0.2mM dNTP mix, 0.5µM of respective gene primers (forward and reverse), 1x Pfu buffer, 8.3ng cDNA template, and nuclease-free water. The PCR program set up was as follows:

Temperature (°C)	95	95	64	72	72	4
Time (s)	120	15	15	30	60	∞
		Cycles: x25 for 18s rRNA, x33 for Gata3, x35 for Tbet				

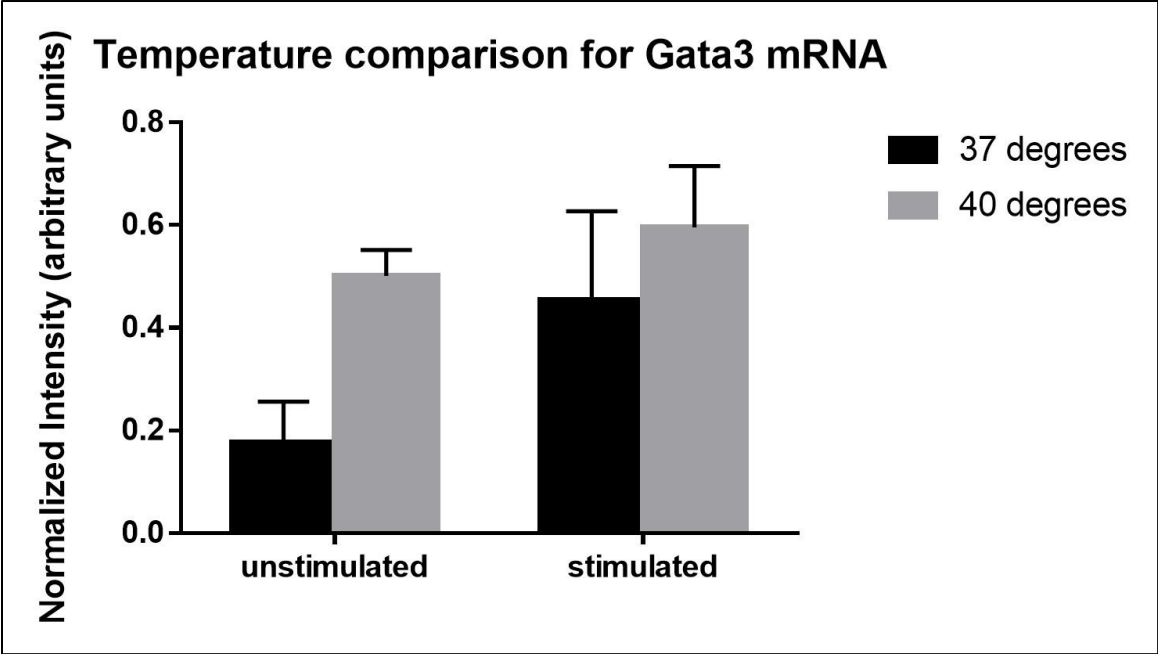
Agarose gel electrophoresis was performed to visualize the PCR products. A 2% agarose (MP Biomedicals, Catalogue no-02100267) gel in 1x TAE was cast. A total of 5µl of the PCR products mixed with 1µl of 6x Cyan-Orange loading dye were then loaded onto the gel, along with a 100bp ladder (ThermoFisher Scientific: Catalogue no-10488058). The gel was run in 1x TAE buffer at a constant voltage of 100V, imaged and analyzed using ImageJ and GraphPad Prism.

RESULTS

Basal expression of Gata3 mRNA in Jurkat cells seems to increase at 40°C:

The 37°C and 40°C unstimulated samples seem to show lower Gata3 expression than the stimulated samples as shown in Figure 13. The 40°C stimulated samples seem to indicate the highest expression of Gata3 amongst all the treatments. The 40°C unstimulated samples seem to show higher expression of Gata3 as compared to the 37°C unstimulated samples. Moreover, the difference between stimulated:unstimulated at 37°C seem to be more than the difference between stimulated:unstimulated at 40°C.

Figure 13: Comparison of Gata3 mRNA levels in 37°C and 40°C Jurkat cells

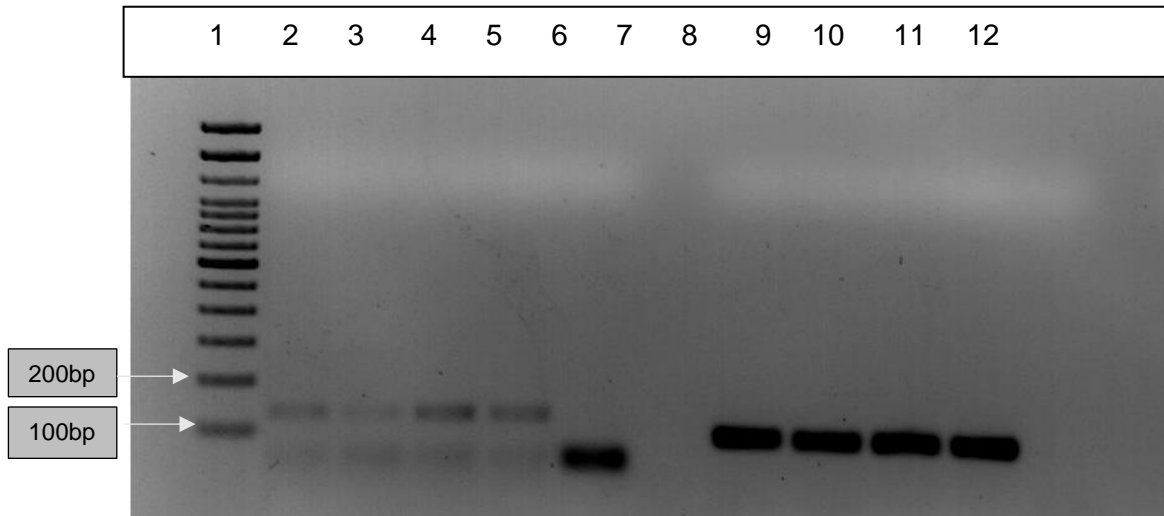


As indicated the y-axis represents normalized arbitrary intensity units. The intensity is normalized by band intensity of 18s rRNA. The x-axis represents the treatment parameter. Each bar is colour coded for the temperature parameter. The mean intensity is plotted and error bars show standard deviation. Here, n=3 biological replicates were used. There was no significant difference in the intensities at 37°C and 40°C.

Even though, visually, from the gel image in Figure 14, it can be seen that the 40°C stimulated and unstimulated Gata3 bands are darker than the 37°C stimulated and

unstimulated, quantitatively this difference is not significant. Thus, these are preliminary indications of differences in Gata3 expression with temperature.

Figure 14: Representative gel image for Gata3 PCR using Jurkat cDNA

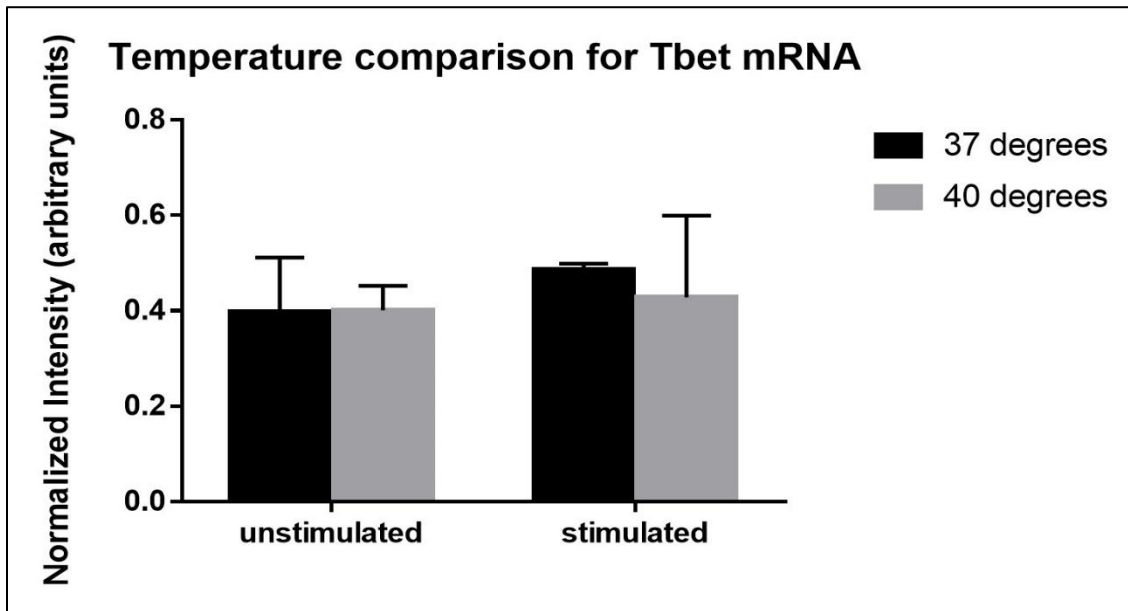


The gel image lane legends are as follows: 1-100bp ladder; 2-37°C stimulated Gata3 band; 3-37°C unstimulated Gata3 band; 4-40°C stimulated Gata3 band; 5-40°C unstimulated Gata3 band; 6-Gata3 NTC band; 7-blank; 8-37°C stimulated 18s rRNA band; 9-37°C unstimulated 18s rRNA band; 10-40°C stimulated 18s rRNA band; 11-40°C stimulated 18s rRNA band; 12-18s rRNA NTC band. The amplicon sizes are indicated in materials and methods along with primer details.

Expression of Tbet mRNA in Jurkat cells seems comparable at 40°C and 37°C:

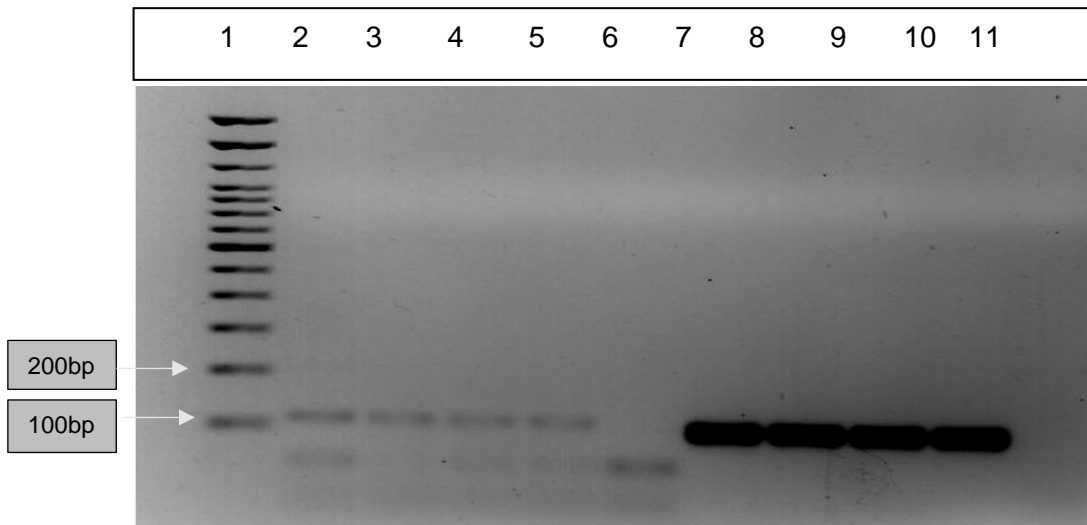
The Tbet expression pattern changes seem to lie within a tighter range as compared to the Gata3 expression pattern. The Tbet expression seems to be highest in the 37°C stimulated condition as seen in Figure 15. The Tbet expression is seemingly lower at 40°C than at 37°C, contrary to the observation in case of Gata3. Even in the unstimulated condition, the basal Tbet level is comparable to the stimulated Tbet expression at both 37°C and 40°C. Moreover, as seen visually from the gel image in Figure 16, all the bands have similar intensities. This tallies up quantitatively as no significant differences in Tbet expression with either stimulation or temperature changes. Thus, more experiments need to be done to confirm these trends.

Figure 15: Comparison of Tbet mRNA levels in 37°C and 40°C Jurkat cells



As indicated the y-axis represents normalized arbitrary intensity units. The intensity is normalized by band intensity of 18s rRNA. The x-axis represents the treatment parameter. Each bar is colour coded for the temperature parameter. The mean intensity is plotted and error bars show standard deviation. Here, n=3 biological replicates were used. There was no significant difference in the intensities at 37°C and 40°C.

Figure 16: Representative gel image for Tbet PCR using Jurkat cDNA



The gel image lane legends are as follows: 1-100bp ladder; 2-37°C stimulated Tbet band; 3-37°C unstimulated Tbet band; 4-40°C stimulated Tbet band; 5-40°C unstimulated Tbet band; 6-Tbet NTC band; 7-37°C stimulated 18s rRNA band; 8-37°C unstimulated 18s rRNA band; 9-40°C stimulated 18s rRNA band; 10-40°C unstimulated 18s rRNA band; 11-18s rRNA NTC band. The amplicon sizes are indicated in materials and methods along with primer details.

DISCUSSION

Naïve T cells have the ability to polarize to either Th1 or Th2 fate depending on the immune priming and cytokine milieu. Tbet and GATA3 are critical transcription factors that drive naïve T cells to Th1 and Th2 phenotypes respectively post stimulation. Previous data in the lab has demonstrated that in ex vivo purified, mouse naïve CD4 T cells; this response seems to be dramatically affected by temperature changes within a tight 0.5°C window of 38.5°C and 39°C (unpublished work). It was observed that there was a Th1 dominant polarization of naïve T cells primed at 37°C (using IFN γ readouts) and a Th2 dominant polarization of naïve T cells primed at 40°C (using IL-13 readouts). These studies also propose that this temperature modulation is regulated via transient receptor potential channels (TRPVs), in particular, TRPV1.

With this background, the current study was undertaken to observe the effects of temperature on human T cells, using Jurkat cell line as a model system. The semi-quantitative data on Jurkat experiments show that there is a change in Gata3 expression at 40°C in both unstimulated and stimulated conditions. Moreover, the corresponding Tbet expression shows no change between 37°C and 40°C. This, however, needs to be quantified using qRT-PCRs, since gel band intensities show a lot of variation. Therefore, in order to evaluate whether the same trend is seen in Jurkats as in mouse T cells, there is a need to quantitatively measure mRNA and protein differences in Gata3 and Tbet with temperature stimulation.

BIBLIOGRAPHY

1. Agrawal, S., and Smith, S.A.B.C. (2013). Transitional B cell subsets in human bone marrow. *J. Transl. Immunol.* 53–59.
2. Amadori, A., and Zamarchi, R. (1995). Genetic control of the CD4/CD8 T cell ratios in humans. *Nat. Med.* 1, 1279–1283.
3. Appenheimer, M.M., Girard, R.A., Chen, Q., Wang, W., Bankert, K.C., Hardison, J., Bain, M.D., Ridgley, F., Sarcione, E.J., Buitrago, S., et al. (2007). Molecular immunology Conservation of IL-6 trans-signaling mechanisms controlling L-selectin adhesion by fever-range thermal stress. *Eur. J. Immunol.* 2856–2867.
4. Basu, S., and Srivastava, P.K. (2003). Fever-like temperature induces maturation of dendritic cells through induction of hsp90. *Japanese Soc. Immunol.* 15, 1053–1061.
5. Bertin, S., Aoki-nonaka, Y., Jong, P.R. De, Nohara, L.L., Xu, H., Stanwood, S.R., Srikanth, S., Lee, J., To, K., Yu, T., et al. (2014). The ion channel TRPV1 regulates the activation and proinflammatory properties of CD4⁺ T cells. *Nat. Immunol.* 15, 1055–1063.
6. Burd, R., Dziedzic, T.S., Xu, Y., Caligiuri, M.A., Subjeck, J.R., and Repasky, E.A. (1998). Tumor cell apoptosis, lymphocyte recruitment and tumor vascular changes are induced by low temperature, long duration (fever-like) whole body hyperthermia. *J. Cell. Physiol.* 177, 137–147.
7. Chen, W., Jin, W., Hardegen, N., Lei, K., Li, L., Marinos, N., McGrady, G., and Wahl, S.M. (2003). Conversion of Peripheral CD4⁺ CD25⁻ Naive T Cells to CD4⁺ CD25⁺ Regulatory T Cells by TGF- β Induction of Transcription Factor *Foxp3*. *J. Exp. Med.* 198, 1875–1886.
8. Choi, S.F. and S.-W. (2005). Gene-Nutrient Interactions in One-Carbon Metabolism. *Curr. Drug Metab.* 6, 37–46.
9. Ciappio, E.D., Mason, J.B., and Crott, J.W. (2011). Maternal one-carbon nutrient intake and cancer risk in offspring. *Nutr. Rev.* 69, 561–571.
10. Evans, D., Frazer, I., and Martin, N. (1999). Genetic and environmental influences on body fat. *Twin Res.* 250–257.
11. Evans, S.S., Wang, W.C., Bain, M.D., Burd, R., Ostberg, J.R., and Repasky, E.A. (2001). Fever-range hyperthermia dynamically regulates lymphocyte delivery to high endothelial venules. *Blood* 97, 2727–2733.

12. Evans, S.S., Repasky, E.A., and Fisher, D.T. (2015). Fever and the thermal regulation of immunity: the immune system feels the heat. *Nat. Publ. Gr.* 15, 335–349.
13. Fontenot, J.D., Gavin, M.A., and Rudensky, A.Y. (2003). Foxp3 programs the development and function of CD4+CD25+ regulatory T cells. *Nat. Immunol.* 4, 330.
14. Fowden, A.L., Giussani, D.A., and Forhead, A.J. (2005). Endocrine and metabolic programming during intrauterine development. *Early Hum. Dev.* 81, 723–734.
15. Fowden, A.L., Ward, J.W., Wooding, F.P.B., Forhead, A.J., and Constancia, M. (2006). Programming placental nutrient transport capacity. *J. Physiol.* 572, 5–15.
16. Harding, J.E., and Johnston, B.M. (1995). Nutrition and fetal growth. *Reprod. Fertil. Dev.* 7, 539–547.
17. Huang, E., and Wells, C.A. (2014). The Ground State of Innate Immune Responsiveness Is Determined at the Interface of Genetic, Epigenetic, and Environmental Influences. *J. Immunol.* 193, 13–19.
18. Jiang, Q., Detolla, L., Singh, I.S., Gatdula, L., Fitzgerald, B., van Rooijen, N., Cross, A.S., and Hasday, J.D. (1999). Exposure to febrile temperature upregulates expression of pyrogenic cytokines in endotoxin-challenged mice. *Am J Physiol* 276, R1653-60.
19. JN, C., Malik, V., Jia, W., and al, et (2009). Diabetes in asia: Epidemiology, risk factors, and pathophysiology. *JAMA* 301, 2129–2140.
20. KAPPEL, M., STADEAGER, C., TVEDE, N., GALBO, H., and PEDERSEN, B.K. (2008). Effects of in vivo hyperthermia on natural killer cell activity, in vitro proliferative responses and blood mononuclear cell subpopulations. *Clin. Exp. Immunol.* 84, 175–180.
21. Lee, J., Breton, G., Yukio, T., Oliveira, K., Zhou, Y.J., Aljoufi, A., Puhr, S., Cameron, M.J., Sékaly, R., Nussenzweig, M.C., et al. (2015). Restricted dendritic cell and monocyte progenitors in human cord blood and bone marrow. *J. Exp. Med.* 212, 385–399.
22. Lillycrop, K.A., Phillips, E.S., Jackson, A.A., Hanson, M.A., and Burdge, G.C. (2005). Dietary protein restriction of pregnant rats induces and folic acid supplementation prevents epigenetic modification of hepatic gene expression in the offspring. *J. Nutr.* 135, 1382–1386.
23. Mace, T. a, Zhong, L., Kokolus, K.M., and Repasky, E. a (2012). Effector CD8+ T cell IFN- γ production and cytotoxicity are enhanced by mild hyperthermia. *Int. J. Hyperth.* 28, 9–18.
24. MacGillivray, D.M., and Kollmann, T.R. (2014). The role of environmental factors in

- modulating immune responses in early life. *Front. Immunol.* *5*, 1–12.
25. Majhi, R.K., Sahoo, S.S., Yadav, M., and Pratheek, B.M. (2015). Functional expression of TRPV channels in T cells and their implications in immune regulation. *FEBS J.* *282*, 2661–2681.
 26. Multhoff, G., Botzler, C., Wiesnet, M., Eissner, G., and Issels, R. (1995). CD3- large granular lymphocytes recognize a heat-inducible immunogenic determinant associated with the 72-kD heat shock protein on human sarcoma cells. *Blood* *86*, 1374–1382.
 27. Orrù, V., Steri, M., Sole, G., Sidore, C., Viridis, F., Dei, M., Lai, S., Zoledziowska, M., Busonero, F., Mulas, A., et al. (2013). Genetic variants regulating immune cell levels in health and disease. *Cell* *155*.
 28. Paparo, L., Di Costanzo, M., Di Scala, C., Cosenza, L., Leone, L., Nocerino, R., and Canani, R.B. (2014). The influence of early life nutrition on epigenetic regulatory mechanisms of the immune system. *Nutrients* *6*, 4706–4719.
 29. Prabhu, S.B., Rathore, D.K., Nair, D., Chaudhary, A., Raza, S., Kanodia, P., Sopory, S., George, A., Rath, S., Bal, V., et al. (2016). Comparison of human neonatal and adult blood leukocyte subset composition phenotypes. *PLoS One* *11*, 1–17.
 30. Rathore, D.K., Nair, D., Raza, S., Saini, S., Singh, R., Kumar, A., Tripathi, R., Ramji, S., Batra, A., Aggarwal, K.C., et al. (2015). Underweight full-term Indian neonates show differences in umbilical cord blood leukocyte phenotype: A cross-sectional study. *PLoS One* *10*, 1–22.
 31. Scott, J.M. (1999). Folate and vitamin B 12 . *Proc. Nutr. Soc.* *58*, 441–448.
 32. Sims, G.P., Ettinger, R., Shirota, Y., Yarboro, C.H., Illei, G.G., and Lipsky, P.E. (2005). Identification and characterization of circulating human transitional B cells. *Blood* *105*, 4390–4398.
 33. Sinclair, K.D., Allegrucci, C., Singh, R., Gardner, D.S., Sebastian, S., Bispham, J., Thurston, A., Huntley, J.F., Rees, W.D., Maloney, C.A., et al. (2007). DNA methylation, insulin resistance, and blood pressure in offspring determined by maternal periconceptional B vitamin and methionine status. *Proc. Natl. Acad. Sci.* *104*, 19351–19356.
 34. Tulapurkar, M.E., Almutairy, E.A., Shah, N.G., He, J.R., Puche, A.C., Shapiro, P., Singh, I.S., and Hasday, J.D. (2012). Febrile-range hyperthermia modifies endothelial and neutrophilic functions to promote extravasation. *Am. J. Respir. Cell Mol. Biol.* *46*, 807–814.
 35. Wang, W., Goldman, L.M., Schleider, D.M., Appenheimer, M.M., Subjeck, J.R.,

- Elizabeth, A., Evans, S.S., Wang, W., Goldman, L.M., Schleider, D.M., et al. (1998). Fever-Range Hyperthermia Enhances L-Selectin-Dependent Adhesion of Lymphocytes to Vascular Endothelium. *J. Immunol.*
36. Wang, X., Ostberg, J.R., and Elizabeth, A. (1999). Effect of Fever-Like Whole-Body Hyperthermia on Lymphocyte Spectrin Distribution, Protein Kinase C Activity, and Uropod Formation. *J. Immunol.*
37. Waterland, R. a, and Jirtle, R.L. (2003). Transposable Elements : Targets for Early Nutritional Effects on Epigenetic Gene Regulation. *Mol. Cell. Biol.* 23, 5293–5300.
38. Yajnik, C.S., Fall, C.H.D., Coyaji, K.J., Hirve, S.S., Rao, S., Barker, D.J.P., Joglekar, C., and Kellingray, S. (2003). Neonatal anthropometry: The thin-fat Indian baby. The Pune maternal nutrition study. *Int. J. Obes.* 27, 173–180.
39. Yajnik, C.S., Deshpande, S.S., Lubree, H.G., Naik, S.S., Bhat, D.S., Uradey, B.S., Deshpande, J.A., Rege, S.S., Refsum, H., and Yudkin, J.S. (2006). Vitamin B12 deficiency and hyperhomocysteinemia in rural and urban Indians. *J. Assoc. Physicians India* 54, 775–782.
40. Yajnik, C.S., Deshpande, S.S., Jackson, A.A., Refsum, H., Rao, S., Fisher, D.J., Bhat, D.S., Naik, S.S., Coyaji, K.J., Joglekar, C. V., et al. (2008). Vitamin B12 and folate concentrations during pregnancy and insulin resistance in the offspring: The Pune Maternal Nutrition Study. *Diabetologia* 51, 29–38.
41. Zhu, J., Yamane, H., and Paul, W. (2010). Differentiation of effector CD4 T cell populations. *Annu Rev Immunol.* 28, 445–489.
42. Zynda, E.R., Grimm, M.J., Yuan, M., Zhong, L., Mace, T.A., Capitano, M., Ostberg, J.R., Lee, K.P., Pralle, A., and Repasky, E.A. (2015). A role for the thermal environment in defining co-stimulation requirements for CD4(+) T cell activation. *Cell Cycle* 14, 2340–2354.